



THE UNIVERSITY *of* EDINBURGH

Edinburgh Research Explorer

## Does soil erosion rejuvenate the soil phosphorus inventory?

**Citation for published version:**

Eger, A, Yoo, K, Almond, PC, Boitt, G, Larsen, IJ, Condrón, LM, Wang, X & Mudd, SM 2018, 'Does soil erosion rejuvenate the soil phosphorus inventory?', *Geoderma*, vol. 332, pp. 45-59.  
<https://doi.org/10.1016/j.geoderma.2018.06.021>

**Digital Object Identifier (DOI):**

[10.1016/j.geoderma.2018.06.021](https://doi.org/10.1016/j.geoderma.2018.06.021)

**Link:**

[Link to publication record in Edinburgh Research Explorer](#)

**Document Version:**

Publisher's PDF, also known as Version of record

**Published In:**

Geoderma

**General rights**

Copyright for the publications made accessible via the Edinburgh Research Explorer is retained by the author(s) and / or other copyright owners and it is a condition of accessing these publications that users recognise and abide by the legal requirements associated with these rights.

**Take down policy**

The University of Edinburgh has made every reasonable effort to ensure that Edinburgh Research Explorer content complies with UK legislation. If you believe that the public display of this file breaches copyright please contact [openaccess@ed.ac.uk](mailto:openaccess@ed.ac.uk) providing details, and we will remove access to the work immediately and investigate your claim.



## Soil erosion and phosphorus

1 **Title:** Does soil erosion rejuvenate the soil phosphorus inventory?

2 **Authors:** Andre Eger<sup>1\*</sup>, Kyungsoo Yoo<sup>2</sup>, Peter C Almond<sup>3</sup>, Gustavo Boitt<sup>3</sup>, Isaac J Larsen<sup>4</sup>, Leo M  
3 Condron<sup>3</sup>, Xiang Wang<sup>2</sup>, Simon M Mudd<sup>5</sup>

4 1 Landcare Research, Department Soil and Landscapes, Gerald St, Lincoln 7608, New Zealand

5 2 University of Minnesota, Department of Soil, Water, and Climate, 439 Borlaug Hall, 1991 Upper  
6 Buford Circle, St. Paul, MN 55108-6028, USA

7 3 Lincoln University, Department of Soil and Physical Sciences, PO Box 85084, Lincoln 7647, New  
8 Zealand

9 4 University of Massachusetts, Department of Geosciences, 627 North Pleasant Street, 233 Morrill  
10 Science Center, University of Massachusetts, Amherst, MA 01003-9297, USA

11 5 University of Edinburgh, School of GeoSciences, Geography Building, Drummond Street,  
12 Edinburgh EH8 9XP, UK

13 \* corresponding author: [egera@landcareresearch.co.nz](mailto:egera@landcareresearch.co.nz), 006433219851

14

15 **Abstract**

16 Phosphorus (P) is an essential nutrient for life. Deficits in soil P reduce primary production and alter  
17 biodiversity. A soil P paradigm based on studies of soils that form on flat topography, where erosion  
18 rates are minimal, indicates P is supplied to soil mainly as apatite from the underlying parent material  
19 and over time is lost via weathering or transformed into labile and less-bioavailable secondary forms.  
20 However, little is systematically known about P transformation and bioavailability on sloping and  
21 eroding hillslopes, which make up the majority of Earth's surface. By linking soil residence time to P  
22 fractions in soils and parent material, we show that the traditional concept of P transformation as a  
23 function of time has limited applicability to hillslope soils of the western Southern Alps (New  
24 Zealand) and Northern Sierra Nevada (USA). Instead, the P inventory of eroding soils at these sites is  
25 dominated by secondary P forms across a range of soil residence times, an observation consistent with  
26 previously published soil P data. The findings for hillslope soils contrast with those from minimally  
27 eroding soils used in chronosequence studies, where the soil P paradigm originated, because  
28 chronosequences are often located on landforms where parent materials are less chemically altered  
29 and therefore richer in apatite P compared to soils on hillslopes, which are generally underlain by pre-  
30 weathered parent material (e.g., saprolite). The geomorphic history of the soil parent material is the  
31 likely cause of soil P inventory differences for eroding hillslope soils versus geomorphically stable  
32 chronosequence soils. Additionally, plants and dust seem to play an important role in vertically  
33 redistributing P in hillslope soils. Given the dominance of secondary soil P in hillslope soils, limits to  
34 ecosystem development caused by an undersupply of bio-available P may be more relevant to  
35 hillslopes than previously thought.

36 **Keywords:** soil phosphorus, phosphorus fractionation, soil residence time, soil age, soil erosion,  
37 hillslopes, soil chronosequences, soil parent material

38

## 39 **Introduction**

40           Phosphorus (P) is an essential element for all life on Earth through its role in forming ATP  
41 and as a structural component of DNA (Nelson et al., 2008). Consequently, the P cycle in terrestrial  
42 and marine environments has been studied extensively (Filippelli, 2002; Paytan and McLaughlin,  
43 2007; Turner and Condron, 2013; Walker and Syers, 1976). Ecological research has shown that P  
44 fertility of terrestrial ecosystems is strongly linked to the weathering trajectory of soils with time: on  
45 geomorphically stable landforms, increasingly chemically altered soils lead to a declining pool of  
46 plant-available P, which can cause a decline of primary production and biomass, and strongly  
47 influence species and functional diversity (Crews et al., 1995; Eger et al., 2013b; Peltzer et al., 2010;  
48 Zemunik et al., 2015). The depletion of plant-available P, however, is not simply a result of P  
49 weathering loss but also due to intensive biochemical transformations and recycling (Frossard et al.,  
50 2000).

51           Our current understanding of long-term P transformations is largely based on soil  
52 chronosequence studies; a study concept that takes advantage of a set of landforms that formed at  
53 different but known times in the past that have been minimally rejuvenated by erosion or deposition.  
54 In this framework, all other soil forming factors since cessation of erosion or deposition are assumed  
55 to have been similar between sites, allowing for isolation of the influence of time on soil  
56 development. Synthesising multiple soil chronosequences in New Zealand, Walker and Syers (1976)  
57 established the seminal soil P development concept: with increasing time, bio-available P declines as  
58 a result of leaching and the transformation of primary, rock-derived apatite P into less directly bio-  
59 available P forms such as organic P and P adsorbed to or occluded into secondary oxides. Whereas  
60 apatite P can be made directly bio-available as  $\text{PO}_4^{3-}$  through mineral dissolution in an acidic soil  
61 environment, the physically occluded P fraction, in particular, comprises P forms that are highly  
62 stabilized (Smeck, 1985) and hence not readily accessible by biota as a result of physical protection in  
63 mineral structures (primary or secondary silicate minerals, oxides, oxyhydroxides), organic matter and

64 soil micro-aggregates (Blake et al., 2003; Guo and Yost, 1998). The Walker and Syers paradigm of P  
65 development has been found to be generally valid for a range of soils in different climatic and  
66 lithologic settings (Crews et al., 1995; Eger et al., 2011; Selmants and Hart, 2010; Turner and  
67 Laliberté, 2015).

68         However, the nominally non-eroding setting of a chronosequence is a special case, as most of  
69 Earth's surface undergoes either net erosion (Larsen et al., 2014b) or deposition. Hillslopes are  
70 predominantly erosional landforms, where gravity and physical disturbances facilitated by water or  
71 bioturbation drive the downslope movement of soil, which is then delivered to fluvial systems or  
72 deposited on convergent sections of slopes or at slope-valley transitions. As mass is physically and  
73 chemically lost from a soil profile on an eroding hillslope, soil cover is maintained over time by the  
74 counterbalancing process of soil production (Gilbert, 1877; Heimsath et al., 1997), the conversion of  
75 parent material to soil. Soil production is regarded as a natural rejuvenator of soil nutrients by the  
76 replacement of weathered, nutrient-poor material with unweathered substrate (Amundson et al., 2015;  
77 Porder and Hilley, 2011; Porder et al., 2007b; Vitousek et al., 2003). The 'fertilisation' through soil  
78 production on slopes could be especially significant for soil P because in most terrestrial settings P is  
79 supplied to the biogeochemical cycle by weathering of the P-bearing mineral apatite and hence is  
80 delivered to the base of the soil by the parent material, unless there are external sources of P, such as  
81 atmospheric input. Dust has a major impact on soil P budgets in sufficiently P-depleted soils and/or  
82 where dust deposition rates are high (e.g., Chadwick et al., 1999; Eger et al., 2013a). Atmospheric  
83 input may even play an important role in P cycling at younger stages of ecosystem development in  
84 some locations (Arvin et al., 2017; Boyle et al., 2013).

85         The role of hillslope topography and soil erosion processes need to be considered when  
86 evaluating soil P pools and fractionation as it will affect the time soil material is residing on the slope  
87 before removal by chemical or physical processes (Agbenin and Tiessen, 1994; Amundson et al.,  
88 2015; Porder and Hilley, 2011; Porder et al., 2007b; Vitousek et al., 2003). For example, in Hawaii  
89 lower proportions of occluded P but more organic P were found on a hillslope in comparison to the  
90 geomorphically stable shield surface, indicating rejuvenation via slope dynamics (erosion and

91 deposition) (Vitousek et al., 2003). However, no clear trends of P fractionation existed across the  
92 hillslope itself, from the shoulder (younger soils) to the toeslope (older soils). P fractionation data  
93 from ridge-slope-valley transects in Puerto Rico demonstrated the dominant control on the spatial  
94 distribution of more labile P forms was topography; labile P was lowest on the ridge and generally  
95 increased downslope towards the valley (Mage and Porder, 2013). In contrast, parent material was the  
96 main control on occluded and total P, with the highest values in the valleys, and apatite P (<5% of  
97 total P in all soils) was unrelated to either topography or parent material (Mage and Porder, 2013).  
98 Selected soil P fractions (total P, apatite P, labile P and occluded P at 0-20 cm depth) on ridgetops in  
99 Puerto Rico were not significantly controlled by erosion rates or soil residence time, however, erosion  
100 rates and residence times varied little between sites (McClintock et al., 2015). Data from slope  
101 transects in Brazil showed that young upper slope soils (Entisols) have higher apatite P and lower  
102 labile P concentrations than Inceptisols in mid and lower slope positions (Agbenin and Tiessen,  
103 1994). Differences in relative soil residence times induced by erosion were deemed the likely reason  
104 for the behaviour of apatite P. With only the study from Brazil adhering to the P-development concept  
105 derived from chronosequences, the relationship between P fractions and the relative soil age on slopes  
106 is less clear.

107         The divergence in P fractionation on eroding slopes relative to what is predicted from  
108 chronosequence studies highlights the need to reconcile the apparently different behaviour of P  
109 observed in different topographic settings. We suggest that comparing these findings in the context of  
110 soil P evolution as proposed by Walker and Syers (1976) is the most promising approach. Amundson  
111 et al. (2015) proposed a unifying concept in which temporal shifts from N to P nutrient limitation in  
112 terrestrial ecosystems are related to the continuum of residence times of minerals within the soil. The  
113 concept of Amundson et al. (2015) builds on new appreciation of tectonic uplift as a driver of erosion  
114 and thus P supply in the otherwise P-depleted tropical soils (Porder et al., 2007b). Uplift is typically  
115 associated with tectonic plate margins and a major control of erosion rates that are inversely related to  
116 soil residence times. Soil residence time in these studies is defined as the length of time that is  
117 required for soil material to be removed by erosion and replaced by soil production, and during which

118 soil particles experience physical and biogeochemical conditions at the top of the weathering profile  
119 (Almond et al., 2007; Dere et al., 2013; McClintock et al., 2015). Compared to chronosequences  
120 developed in flat landforms, Amundson et al. (2015) suggested that residence times for most hillslope  
121 soils in temperate climates give rise to neither N nor P limitation. In other words, soils on eroding  
122 hillslopes are not too young to have N limitation or too old to be depleted in mineral P.

123         Whether eroding hillslope soils indeed occupy an optimal residence time window with respect  
124 to P limitation remains to be tested. There are few data that directly link individual P fractions to  
125 absolute soil residence times (McClintock et al., 2015). Additionally, previous studies of soil P on  
126 eroding hillslopes are largely limited to tropical landscapes (Abekoe and Tiessen, 1998; Agbenin and  
127 Tiessen, 1994; Araújo et al., 2004; Mage and Porder, 2013; McClintock et al., 2015; Porder and  
128 Hilley, 2011; Porder et al., 2007b; Vitousek et al., 2003). In these actively eroding tropical systems,  
129 deep chemical alteration of bedrock causes soils to be depleted in apatite P, which provides the first  
130 indication that the optimal window hypothesis may not be applicable globally. However, the  
131 applicability of these studies from tropical landscapes to extra-tropical regions may also be limited. In  
132 contrast to temperate climate regions, in the tropics, deep and more completely weathered profiles  
133 prevail, mineralisation rates of organic matter are higher, low-reactivity clays and pedogenic  
134 oxide/hydroxides increasingly dominate the residual soils, and the legacy of glacial/periglacial  
135 conditions during the Pleistocene is largely absent.

136         Here we present new P fractionation data quantitatively linked to hillslope soil residence  
137 times across two gradients of erosion rates in temperate ecosystems and compare them to published  
138 results regarding patterns and rates of P transformation. We initially hypothesised, based on the  
139 proposal by Amundson et al. (2015), that higher soil production and erosion rates and hence shorter  
140 residence times result in high total soil P concentrations and high proportions of primary mineral P as  
141 expected for immature soils, whereas lower erosion rates and longer residence times result in low total  
142 soil P due to the intensive weathering of older soil particles, and a high proportion of secondary P  
143 forms as expected in more mature soils. However, our data do not support this hypothesis and instead,  
144 somewhat distinct from the conceptual framework laid out in Walker and Syers (1976), highlight the

145 significance of weathering below the base of the soil in temperate climates, biological uptake of P and  
146 potential dust accretion.

## 147 **Methods**

### 148 **Definition of mean soil particle age, residence time, turnover time and comparison with soil age**

149 We first require a consistent framework for the measure of time for our soils. As we will  
150 show, soil residence time and soil age provide consistent temporal references to which soil P  
151 dynamics from geomorphically active and stable landscapes can be compared. We conceptualize that  
152 the mass balance of a hillslope soil (Fig. 1) is largely determined by the difference between the mass  
153 losses via physical and chemical erosion and mass input via soil production; our conceptualization  
154 assumes aeolian inputs are negligible. In this simplified view, a hillslope soil is defined as a part of a  
155 weathering profile that has been not only chemically weathered but also physically disturbed and  
156 mixed. In contrast, the lower part of the weathering profile is considered chemically weathered but  
157 physically undisturbed (i.e., saprolite). We assume soil mass removal via physical and chemical  
158 erosion is balanced by soil production, such that a steady-state is reached (Heimsath et al., 1997).  
159 Since our focus is on transformations and losses of P in hillslope soils (i.e., soil as the residual of the  
160 weathering process), we are concerned with the ages of the particles with respect to their initial  
161 incorporation within the soil, as exposure to weathering and leaching increases as a function of  
162 particle age. Hillslope soil particles have a distribution of age that is unknowable in all but the  
163 simplest case of steady state soil thickness, together with either complete mixing or plug flow (Mudd  
164 and Yoo, 2010) and the absence of chemical weathering. Hence, pragmatically, we seek only a metric  
165 to rank soils according their exposure to weathering. Under aforementioned simplifying conditions,  
166 mean particle age of the soil ( $\psi$ ), mean soil residence time ( $\chi$ , average age of particles leaving the soil)  
167 and soil turnover time ( $\phi$ , the length of time that it takes for a soil particle to be completely depleted  
168 by the outgoing flux) are equal (Almond et al., 2007; Mudd and Yoo, 2010; Yoo and Mudd, 2008).  
169 We adopt the mean particle age, and, assuming perfect mixing and steady state in the absence of  
170 chemical weathering, we estimate it by the soil turnover time. Soil turnover time is calculated as the



171 ratio of the mass of the soil and the outgoing mass flux from that soil (Mudd and Yoo, 2010).  
 172 Assuming steady state, the outgoing mass flux (erosion) equals the rate of conversion of parent  
 173 material to soil (i.e., soil production rate) as determined by cosmogenic nuclide measurements at each  
 174 of our sites (see below) corrected for chemical mass loss.

$$175 \quad \psi = \varphi = \chi = \frac{[Zr]_s \rho_s h}{[Zr]_r \rho_r D} \quad \text{equation (1)}$$

176 where  $\psi$  is mean particle age,  $\varphi$  residence time and  $\chi$  is turnover time (T).  $[Zr]$  represents the  
 177 mass concentration of the immobile element zirconium ( $\text{MM}^{-1}$ ),  $\rho$  is bulk density ( $\text{ML}^{-3}$ ),  $h$  is soil  
 178 thickness (L),  $D$  is soil production/erosion rate ( $\text{LT}^{-1}$ ), and subscripts  $s$  and  $r$  indicate soil and parent  
 179 material, respectively. The term  $[Zr]_s/[Zr]_r$  converts the soil erosion rate, which includes a chemical  
 180 weathering component, into a physical erosion rate (e.g., Riebe et al., 2003). Since soil thickness and  
 181 soil production rate units are given in length, the inclusion of  $\rho_s/\rho_r$  accounts for the dilation between  
 182 parent material and soil. Here  $[Zr]_s/[Zr]_r$  is typically larger than 1 because of Zr enrichment in soils as  
 183 a result of leaching of other more soluble elements. In contrast, the bulk density ratio between soils  
 184 and the parent material is typically less than 1, contributing to cancelling the effect of Zr enrichment  
 185 in soils. Thus we further simplify our soil particle age metric to  $h/D$ , similar to other studies (e.g.,  
 186 Amundson et al., 2015; Porder et al., 2007b). In the literature, mean soil particle age, mean soil  
 187 residence time, or soil turnover time have been used interchangeably or authors simply referred to soil  
 188 residence time without strict definitions based on reservoir theory (e.g., Almond et al., 2007;  
 189 Amundson et al., 2015; Green et al., 2006; Porder and Hilley, 2011). We follow this convention and  
 190 use the term soil residence time instead of the mean particle age or turnover time.

191 While an approximate steady state is a useful concept for investigating eroding soils, soils developing  
 192 on geomorphically stable landforms are only minimally affected by physical erosion. Still, a mean age  
 193 of soil mineral particles can be defined (Yoo and Mudd, 2008). A soil consists of mineral particles  
 194 that have a range of time lengths (i.e., ages) since their physical incorporation into the soil from the  
 195 underlying parent materials. The maximum age of mineral grains cannot be older than the age of the  
 196 soil, however. Soil age is defined as time length since cessation of erosion or deposition. Additionally,

197 in non-eroding chronosequences, soils become increasingly thicker with time as chemically more inert  
198 soil material residually accumulates, which slows the downward propagation of soil development into  
199 the parent material (Lebedeva et al., 2010), and hence the rate of incorporation of nutrient-  
200 replenishing parent material (Yoo and Mudd, 2008). Thus, the number of mineral grains introduced to  
201 the soil from the underlying parent material exponentially decreases over time. As a consequence, it is  
202 expected that the mean age of the mineral particles is less than soil age, but the distribution of  
203 individual mineral grains' ages is skewed toward the early phase of soil formation. Thus, the mean  
204 age of mineral grains in a soil is proportional to the soil age (Yoo and Mudd, 2008).

### 205 *Study site and field sampling*

206 The P data come from two temperate locations that differ substantially in rainfall and soil  
207 production/erosion rates. Soil thicknesses, soil production/erosion rates, and calculated soil residence  
208 times (Eq. 1) for each soil are reported in Tables 1 and 2. Soil thicknesses and soil production/erosion  
209 rates were reported previously and the methods and discussion concerning these data, and the range of  
210 parameters are described by Larsen et al. (2014a) for the Western Southern Alps (WSA) sites, and  
211 Hurst et al., (2012) and Yoo et al. (2011) for the Feather River (FR) sites. Soil residence times at FR  
212 sites were also reported in Wang et al. (2018).

213 The first study area is located in the western Southern Alps (WSA) of New Zealand at the  
214 collisional boundary of the Australian and Pacific Plates (Fig. 2), resulting in up to 10 mm y<sup>-1</sup> tectonic  
215 uplift (Little et al., 2005; Tippett and Kamp, 1993). Soil parent material is schist derived from a  
216 greywacke protolith. The Southern Alps form an orographic barrier against the prevailing westerly  
217 airstream resulting in a mean annual precipitation of 10391 mm (1979-2015, maximum Dec 1099  
218 mm, minimum July 643 mm), with a mean annual temperature of 5.5°C (NIWA, 2016; Tonkin and  
219 Basher, 2001) at ~900 m asl. The natural vegetation cover is a podocarp-hardwood forest and  
220 subalpine, dense scrub/low tree communities (Wardle, 1977). Topography is heavily dissected by a  
221 dense drainage network of steep, V-shaped valleys including waterfalls, gorges, and narrow ridge  
222 lines (Whitehouse, 1988). Landslides are frequent as a result of earthquakes and high rainfall (Hilton

223 et al., 2008; Hovius et al., 1997; Korup et al., 2004), but return intervals are long enough to allow the  
224 formation of thin soil and regolith cover at any point on the landscape between failures (Larsen et al.,  
225 2014a; Whitehouse, 1988).

226 The soil production/erosion rates in the WSA (Table 1) are amongst the highest in the world  
227 (Larsen et al., 2014a) and the soils are weakly developed Entisols or Inceptisols (Soil Survey Staff,  
228 2014). All individual soil sampling sites were located on the main ridges or in local, meter-scale  
229 convexities on smaller divides emanating from the main ridges to avoid effects from landsliding. As  
230 such the site selection aimed at fulfilling the steady state assumption required by the *in-situ*  
231 cosmogenic nuclide method to yield reliable soil production rates at each site. We do not necessarily  
232 expect these sites to be representative of the average soil thickness in each of the WSA catchments.  
233 Local slope at the soil sites ranged between 24° to 50°.

234 The second study area is in the Feather River catchment (FR) in the Northern Sierra Nevada  
235 of California, USA (Fig. 2). The FR site is within the lower reaches of the Middle Fork Feather River,  
236 where mean annual precipitation is 1750 mm and the mean annual temperature 12.5 C° (PRISM  
237 Climate Group, [www.prism.oregonstate.edu](http://www.prism.oregonstate.edu)). The bedrock at the study site is granodiorite, but the  
238 adjacent area features a complex intrusion of granitoid plutons into metamorphic and ophiolitic rocks  
239 (Saucedo and Wagner, 1992). Erosion rates vary with topography, with lower erosion rates of 20-40  
240 mm ky<sup>-1</sup> for a relatively flat relict upland surface and high erosion rates of 200-250 mm ky<sup>-1</sup> on the  
241 steep slopes draining to the deeply incised canyon of the Feather River (Hurst et al., 2012; Riebe et  
242 al., 2000; Wakabayashi and Sawyer, 2001).

243 The FR study sites are located within the Bald Rock tributary basin that descends from a relict  
244 surface (850 m asl) to the Middle Fork Feather River (310 m asl). Spatially detailed rainfall data are  
245 lacking in the region. However, the region's precipitation map (Western Regional Climate Center,  
246 <https://wrcc.dri.edu/Climate/maps.php>) suggests that the elevation difference within the tributary  
247 basin causes only ~15% of variation in the annual mean precipitation. Relatively constant climate  
248 within the basin is also reflected in homogenous presence of mixed conifer forest (Milodowski et al.,

249 2014). The overall slope gradients of the FR sites within the tributary basin increase from  
250 approximately 15° to 31° toward the Middle Fork Feather River. A knick-point, which has been  
251 initiated by the incision of the Middle Fork Feather River, has been migrating upward through the  
252 tributary basin (Attal et al., 2015). Our sites comprise three eroding hillslope transects: POMD is near  
253 a low relief plateau and located above the knick-point, BRC is below the knick-point, and FTA is  
254 between the knick-point and the plateau. According to Hurst et al. (2012), catchment scale erosion  
255 rates adequately represent the spatial variability of erosion rates within the tributary basins and vary  
256 from 35.7 mm ky<sup>-1</sup> at POMD to 250 mm ky<sup>-1</sup> at BRC, with intermediate rates at the FTA sites. Since  
257 the soil thicknesses of the FTA soils do not differ significantly from those of POMD and BRC, they  
258 will have soil residence times that are between those of POMD and BRC (Table 2). Consistent with  
259 the range of residence times, all soils are Inceptisols. The BRC soils with highest erosion rates have  
260 substantially more coarse grain sizes and are more heterogeneous in their thicknesses as compared to  
261 POMD and FTA (Wang et al., 2018). Unlike POMD and FTA, which have continuous soil cover,  
262 BRC is also characterized by patchy bedrock outcrops (Milodowski et al., 2015). Though a generally  
263 negative relationship between soil thickness and erosion rate has been observed at an adjacent ridge  
264 line (Gabet et al., 2015), within the Bald Rock Basin soil thickness is relatively insensitive to erosion  
265 rate (Yoo et al., 2011).

266 With respect to our conceptual framework of hillslope soils (Fig. 1), we define soil as the sum  
267 of pedogenic A and B horizons (Soil Survey Staff, 2014). Our field observations clearly indicated the  
268 effects of physical disturbance by tree roots and tree throws in mixing these horizons, qualifying the  
269 sum of A and B horizons as the mobile soil. The zone of chemical weathering between the soil and  
270 fresh bedrock, which is termed saprolite (Fig. 1), is characterised in our study areas by well-preserved  
271 rock fabric indicative of minimal physical disturbance. At WSA, the thin (<0.5 m) saprolite zone can  
272 be at times better described as R horizon that comprises in-situ (i.e., physically connected to bedrock  
273 below), minimally weathered bedrock, and mm-sized cracks containing material from the overlying B  
274 horizon. At the WSA sites we took bulk-samples (combined A and B horizons) of each soil profile  
275 (one sample per site, total 22 samples from 22 soil sites). We took great care to obtain bulk samples

276 that represented the true proportions of each soil horizon in the soils (i.e., no preferential sampling of  
277 one horizon) by cutting back the profile face with a spade over the entire depth of the soil and  
278 collecting the cut-back material. At the FR site each hillslope (POMD, FTA, BRC) was sampled at the  
279 summit, shoulder, and backslope for soil and saprolite material (convex to straight slopes). Each soil  
280 pit was excavated to the depth of 20-30 cm below the soil-saprolite boundary and soil samples were  
281 collected by horizons and depth intervals. Because little differences in soil geochemistry and  
282 morphology were observed as a function of topographic locations within each hillslope group (Yoo et  
283 al., 2011), our detailed P fractionation measurements were limited to two soil profiles from each  
284 hillslope.

### 285 *Laboratory methods*

286 We primarily present P data of soil samples and saprolite (FR only) for the following fractions:  
287 total P ( $P_{\text{total}}$ ), the primary, apatite-derived P fraction ( $P_{\text{apatite}}$ ), organic P as the organically bound P  
288 ( $P_{\text{org}}$ ), the non-occluded, iron and aluminium oxide-bound P ( $P_{\text{Fe/Al}}$ ), and the  
289 occluded/recalcitrant/residual P fraction ( $P_{\text{occ}}$ ). The extraction procedures differed between the WSA  
290 and FR sites due to the dates when the analyses were conducted (WSA in 2013, FR in 2016). For the  
291 WSA sites,  $P_{\text{total}}$  was extracted by NaOH fusion in nickel crucibles (Blakemore et al., 1987; Smith and  
292 Bain, 1982), and the extracts analysed following Murphy and Riley (1962).  $P_{\text{org}}$  was extracted  
293 following the ignition method of Saunders and Williams (1955). The modified Hedley sequential  
294 fractionation with 0.1M NaOH and 1M HCl after Tiessen and Moir (1993) yielded inorganic  $P_{\text{Fe/Al}}$   
295 and  $P_{\text{apatite}}$ , respectively.  $P_{\text{org}}$ ,  $P_{\text{Fe/Al}}$ , and  $P_{\text{apatite}}$  extracts were quantified also following Murphy and  
296 Riley (1962). The difference between total P and the sum of  $P_{\text{org}}$ ,  $P_{\text{apatite}}$ , and  $P_{\text{Fe/Al}}$  is regarded as the  
297 occluded/recalcitrant/residual P ( $P_{\text{occ}}$ ). We note that our  $P_{\text{occ}}$  fraction does not discriminate between  
298 inorganic and organic  $P_{\text{occ}}$ .

299 The FR samples underwent a more detailed fractionation than the WSA samples following the  
300 scheme by Condron et al. (1996). This scheme involves a sequential extraction of 6 consecutive steps  
301 on the same soil sample: 1) extraction of labile inorganic P with 1M ammonium chloride ( $P_{\text{NH}_4\text{Cl}}$ ); 2)

302 inorganic and organic P ( $P_{\text{bic}}$  and  $P_{\text{obic}}$ ) with 0.5M sodium bicarbonate ( $\text{NaHCO}_3$  at pH 8.5); 3)  
303 inorganic and organic P ( $P_{\text{OH}_I}$  and  $P_{\text{OOH}_I}$ ) with 0.1M NaOH; 4)  $P_{\text{apatite}}$  ( $P_{\text{HCl}}$ ) with 1M HCl; 5) a  
304 second extraction with 0.1M NaOH ( $P_{\text{OH}_II}$  and  $P_{\text{OOH}_II}$ ); and a final digestion with concentrated  
305  $\text{H}_2\text{SO}_4$  and 30%  $\text{H}_2\text{O}_2$  to yield the residual P (Olsen and Sommers, 1982). The inorganic P  
306 concentration in acid extracts was quantified following Murphy and Riley (1962). Inorganic P in  
307 alkaline extracts followed Dick and Tabatabai (1977), whereas the organic P was obtained by the  
308 difference between the inorganic P and total P concentrations after digestion with ammonium  
309 persulfate and  $\text{H}_2\text{SO}_4$  in an autoclave.

310 To allow for comparability, the FR P fractions were combined to be equivalent to the WSA  
311 fractions: organic P ( $P_{\text{org}}$ ) is the sum of  $P_{\text{obic}}$ ,  $P_{\text{OOH}_I}$  and  $P_{\text{OOH}_II}$ ; apatite P ( $P_{\text{apatite}}$ ) is equivalent to  
312  $P_{\text{HCl}}$ ;  $P_{\text{Fe/Al}}$  is  $P_{\text{OH}_I}$ ; and occluded P ( $P_{\text{occ}}$ ) equals the sum of  $P_{\text{OH}_II}$  and  $P_{\text{residual}}$  (here we account for  
313 the fact that the simpler P fractionation of the WSA samples does not include a second NaOH  
314 extraction that was performed on the Feather River samples). P data are only reported for the mineral  
315 horizons (Table 1 for WSA and Table 2 for FR). At both sites we measured pH of the bulk samples  
316 (WSA) and selected depth increments (FR) at a soil/water mass ratio of 1:2.5. To compare results  
317 between the two sites and previous work, we focus on the ratios of  $P_{\text{apatite}}$ ,  $P_{\text{occ}}$ ,  $P_{\text{org}}$ , and  $P_{\text{Fe/Al}}$  to  $P_{\text{total}}$   
318 rather than absolute P concentrations, as this approach allows comparison of sites with varying  
319 concentrations of P in the parent material (Hahm et al., 2014; Mage and Porder, 2013; Porder and  
320 Ramachandran, 2013). Regression analysis and derivation of regression model parameters was  
321 conducted using R (R Core Team 2017).

## 322 **Results**

### 323 *Western Southern Alps, New Zealand*

324 Soils are very acidic (Table 1) with pH values as low as 3.2, similar to other published data  
325 from the region (e.g., Almond and Tonkin, 1999; Stevens 1968; Tonkin and Basher, 2001). Since  
326 these are composite values representing the substrate over the entire depth of each soil, the values are  
327 likely to be lower for the topsoils and higher for the subsoils alone. Secondary P is the predominant

328 form of P in the WSA samples (83-97%), whereas apatite P remains between 3% to 17% of  $P_{total}$  over  
329 the entire range of soil residence times (Fig. 3, Table 1). The  $P_{apatite}/P_{total}$  ratio is weakly inversely  
330 correlated with soil residence time ( $\chi$ ) ( $P_{apatite}/P_{total}=0.1144^{-0.0002\chi}$ ,  $R^2=0.18$ ,  $p=0.045$ ). In contrast,  
331 neither  $P_{org}$  nor P mainly associated with pedogenic oxides ( $P_{occ}$  and  $P_{Fe/Al}$ ) are statistically  
332 significantly correlated with residence time.

### 333 *Feather River, California, USA*

334 Soils at FR are slightly acidic throughout. At the FR sites (Fig. 3), depth-weighted  
335 contributions of P fractions to  $P_{total}$  of each soil show  $P_{apatite}$  is always <3% of  $P_{total}$ , whereas  $P_{org}$  and  
336  $P_{occ}$  are clearly dominant. The high proportions of  $P_{org}$  and  $P_{occ}$  are present across the range of soil  
337 residence times (Fig. 3). Only  $P_{org}$  decreases slightly with increasing soil residence time ( $\chi$ ) following  
338 a statistically significant power-law model ( $P_{org}/P_{total}=0.76\chi^{-0.113}$   $R^2=0.89$ ,  $p<0.005$ ). Since P fractions  
339 are measured in consecutive depth intervals and soils are deeper at the FR sites than the WSA sites, a  
340 more detailed picture of the P fractions across soil depths was obtained (Fig. 4). Despite the  
341 rudimentary morphological development of the Inceptisols, there are major depth gradients in P  
342 chemistry. Nearly all P fractions and  $P_{total}$  have highest concentrations in the topsoil (Fig. 4, Table 2).  
343 High topsoil concentrations are most strongly expressed in the more bio-available secondary forms of  
344 P ( $NH_4Cl$ ,  $NaHCO_3$ , and first NaOH extractions) but also  $P_{apatite}$ . The decline for most P fractions with  
345 depth continues beyond the soil and reaches deep (>200 cm) into the saprolite (Cr) with the exception  
346 of  $P_{apatite}$  concentrations, which increase again in concentration at depths >150 cm.

## 347 **Discussion**

### 348 *Soil P relative to soil residence time vs. soil age*

349 Soil residence times vary by up to four orders of magnitude but residence times exert little  
350 control on the concentrations of total P;  $P_{apatite}/P_{total}$  ratios remain low (<18% at WSA, <3% at FR) for  
351 all soils (Table 1 and 2). The statistically significant model linking soil residence time to  $P_{apatite}/P_{total}$ ,  
352 albeit statistically weak, indicates that the paradigm of  $P_{apatite}$  loss with increasing soil development

353 time cannot be rejected at least for WSA. However, at WSA the proportion of  $P_{\text{apatite}}$  to  $P_{\text{total}}$  at the  
354 shortest soil residence time is <18% in contrast to the classic Walker & Syers paradigm that predicts  
355 the dominance of  $P_{\text{apatite}}$  over secondary P forms in such young soils with rudimentary profile  
356 morphology (Entisols, Inceptisols).

357 In Fig. 5, we compared our own ratios of  $P_{\text{apatite}}/P_{\text{total}}$  as a function of soil residence time to the  
358 published ratios from soil chronosequence studies. It appears that soils at both of our study sites,  
359 despite not being morphologically developed beyond Inceptisols, have already reached the late stage  
360 of soil P development with a very low and largely invariant proportion of  $P_{\text{apatite}}$  and very high  
361 secondary P forms typical for older chronosequence sites (Fig. 5). For instance, contrasting the WSA  
362 sites against the Spodosols developed on the nearby Franz Josef chronosequence shows that the 10%  
363 average proportion of  $P_{\text{apatite}}$  in the WSA soils is at best similar to the top 30 cm (to stay within our  
364 range of WSA soil depths) of >1000- to 5000-year-old soils of the Franz Josef chronosequence  
365 (Stevens, 1968). Additionally, the  $P_{\text{occ}}/P_{\text{total}}$  ratios of the hillslope soils at WSA are so high that they  
366 are only replicated at the 120,000 y-old, retrogressive stage of the Franz Josef chronosequence (data  
367 from Stevens, 1968).

368 Contrasting the FR sites to the Merced River chronosequence (Harden, 1987), developed on  
369 granite-derived alluvium and located just west of the Sierra Nevada, reveals that, like the WSA, the P  
370 chemistry of hillslope soils is comparable to that of old soils. We note here that the Merced River sites  
371 developed in a dryer climate than the FR sites (mean annual precipitation: 300 mm). Although P  
372 fractionation data are not available for the Merced River chronosequence, the site's apatite  
373 concentrations can serve as a proxy for the depletion of primary mineral P ( $P_{\text{apatite}}$ ) (Harden, 1987).  
374 Apatite concentrations in Merced River soils decrease 10-fold within the first 40 ky of soil formation  
375 with little change thereafter (>40 ky to 600 ky). The initially rapid decline of apatite observed at the  
376 Merced River chronosequence is similar to the trend in  $P_{\text{apatite}}$  depletion at Franz Josef and other  
377 chronosequences (Fig. 5). Comparing the FR sites to Merced River chronosequence, the low and  
378 invariant contributions of  $P_{\text{apatite}}$  to  $P_{\text{total}}$  at the FR site signals that FR soils have already reached that  
379 stage of severe apatite depletion only observed in Merced River soils older than 40 ky that exhibit



380 much greater morphological maturity and chemical differentiation (e.g. layers of illuvial clay-  
 381 enrichment in the soil) than the FR hillslope soils.

382 The only other published P fractionation data in Fig. 5 from eroding hillslopes with temporal data are  
 383 from Puerto Rico (McClintock et al., 2015). McClintock et al. (2015) reported soil residence time for  
 384 the top 20 cm of soils and every sample contained less than 5% of  $P_{\text{apatite}}$  (their HCl-extractable P).  
 385  $P_{\text{occ}}$  (residual-P),  $P_{\text{org}}$  ( $\text{NaHCO}_3\text{-P}_o + \text{NaOH-P}_o$ ) and  $P_{\text{Fe/Al}}$  ( $\text{NaOH-P}_1$ ) contribute on average 55%,  
 386 30%, and 13% to  $P_{\text{total}}$ , respectively. The residence times of their soils are comparable to those we  
 387 studied (Fig. 5), and there is also similarity to our average P inventory that shows the contributions to  
 388  $P_{\text{total}}$  of  $P_{\text{occ}} > P_{\text{org}} = P_{\text{Fe/Al}}$  for WSA and  $P_{\text{occ}} > P_{\text{org}} > P_{\text{Fe/Al}}$  for FR (Fig. 3). These similar patterns in soil  
 389 P persist despite the large climatic difference between WSA, FR and Puerto Rico (Fig. 6), indicating  
 390 that climate is not a driver of such patterns observed in P fractions.

### 391 *Comparison to published soil P data from eroding hillslopes*

392 Our results differ from the patterns reported for soil chronosequence studies (Fig. 5) but are  
 393 consistent with soil P fractionation studies conducted on eroding hillslopes underlain by crystalline  
 394 bedrock (Fig. 7). These published data are compiled from studies that explicitly describe soil  
 395 sampling locations on hillslopes and from in-situ soil parent materials (or local regolith). Most sites in  
 396 Fig. 7 are upslope locations where soil production from the underlying bedrock maintains soil cover  
 397 and colluvial deposition is limited. All soils from eroding hillslopes in the published literature, despite  
 398 their presumably short soil residence times due to erosion, have very low percentages of  $P_{\text{apatite}}$  (Fig.  
 399 7). Eroding soils also contain a high proportion of  $P_{\text{occ}}$  relative to  $P_{\text{total}}$  (Abekoe and Tiessen, 1998;  
 400 Araújo et al., 2004; Homyak et al., 2014; Mage and Porder, 2013; McClintock et al., 2015; Vitousek  
 401 et al., 2003), consistent with results from the WSA and FR sites.

402 In Fig. 7, the soils from semi-arid northern Brazil (Agbenin and Tiessen, 1994) are an  
 403 exception to the low contribution of  $P_{\text{apatite}}$  to  $P_{\text{total}}$  in eroding soils. The  $P_{\text{apatite}}$  contribution to  $P_{\text{total}}$  in A  
 404 horizons of these upslope soils reaches  $60 \pm 18\%$  in shallow Entisols, but that quickly decreases to  
 405  $17 \pm 18\%$  lower on the slope where thick depositional Inceptisols are found. However, this northern

406 Brazilian hillslope (Agbenin and Tiessen, 1994) is underlain by apatite-rich syenite that is unusual for  
407 the region (Araújo et al., 2004). In summary, excluding the study site underlain by apatite-rich  
408 syenite, no previous work from eroding hillslopes we examined documents  $P_{\text{apatite}}$  contributing  $>30\%$   
409 of  $P_{\text{total}}$ .

410 Despite the extreme rainfall rates, it seems unlikely that the strong depletion of  $P_{\text{apatite}}$  at WSA  
411 is simply a reflection of the high rainfall in accelerating the weathering and transformation of  
412 rock/soil P. Fig. 7 shows the range of precipitation from the published hillslope P studies including  
413 those from this study. It is clear that the exceedingly low contribution of apatite to total P on eroding  
414 hillslopes is not limited to regions of high rainfall but rather is a norm across a wide range of  
415 precipitation rates.

416 Although they did not measure phosphorus, Dixon et al. (2009) linked erosion rates and  
417 chemical weathering state of soils and saprolite. They found that the chemical weathering state of the  
418 saprolite determined the chemical weathering of the soil: when the saprolite was highly weathered,  
419 additional weathering in the soil was low, whereas when the saprolite was only weakly chemically  
420 altered, the contribution of soil weathering to the overall chemical weathering of the weathering  
421 column would be high. Given that Dixon et al. (2009) found a strong relationship between erosion  
422 rate and weathering rate of the saprolite (but not the soil), we expected that the P inventory of the  
423 saprolite at FR would respond to erosion rates. However, this (i.e., higher erosion rates/lower  
424 residence times = less strongly depleted apatite P in the saprolite) does not seem to be the case at FR  
425 (see saprolite samples in Table 2).

#### 426 ***Potential effects of aeolian P input***

427 One potential contribution to the P depth profiles we see (e.g., the increase in total P from  
428 saprolite to soil observed at FR; Fig. 4) is dust deposition. Substantial dust deposition is highly  
429 unlikely for the WSA sites, as studies have shown that even in favourable conditions of local dust  
430 mobilisation (e.g. close to an unvegetated braided river in the coastal plain) any effect of dust on soil  
431 P is limited to areas close to the dust source ( $<2$  km) (Eger et al., 2013a). There is no local dust-

432 producing source in the vicinity of our WSA sites and long-range deposition from Australia  
433 (Holocene dust deposition rate  $0.6 \text{ g m}^{-2} \text{ y}^{-1}$ ; Marx et al., 2009) will have little impact at such high  
434 erosion rates (lowest rate of all WSA soils  $307 \text{ g m}^{-2} \text{ y}^{-1}$ ; Larsen et al., 2014a). For the FR sites, as  
435 indicated by the peaks of most P fractions and  $P_{\text{total}}$  in the topsoil, deposition of dust may be more  
436 significant even in eroding (and thus rejuvenating) soils. Aciego et al. (2017) extrapolated a three-  
437 month dust trapping record from the driest months in the Sierra Nevada to annual deposition rates of 3  
438 to  $36 \text{ g m}^{-2}$ . Hence, although this extrapolation might be an overestimation due to limiting the  
439 measurements to the dry season, we acknowledge the likely accretion of P-bearing dust in the FR  
440 study area. However, dust deposition has little effect on our interpretation. With increasing soil depth,  
441 closer to the parent material source, and decreasing potential impact of atmospheric deposition, the  
442  $P_{\text{apatite}}$  remains low and secondary P forms remain clearly dominant regardless of soil residence time  
443 (Fig. 4). Alternative or complementary explanations for the surface peak in P concentrations include P  
444 uplift by plants (Jobbágy and Jackson, 2004) or bioturbation within the soil (e.g., frequently observed  
445 tree throw in the study area).

#### 446 *Soil P and soil order*

447 All of the soils at our field sites are either Entisols or Inceptisols. Nevertheless, they are  
448 highly depleted in  $P_{\text{apatite}}$ . Our data are largely consistent with other soil P studies conducted for  
449 eroding hillslopes (Fig. 8a). These observations clearly deviate from the general relationship of P  
450 fractions and soil orders postulated first by Smeck (1985), which is a pedological extension of the  
451 Walker and Syers (1976) paradigm, such that the progressive change of soil orders is aligned with the  
452 predictable changes in soil P. Soils are assumed to develop in a sequence from Entisols to Inceptisols  
453 to Alfisols to Ultisols (or Spodosols) to Oxisols (Smeck, 1985). The concept of correlation between  
454 soil P fractions and soil orders was later confirmed through global data compilations (Cross and  
455 Schlesinger, 1995; Lajtha and Schlesinger, 1988; Yang and Post, 2011). However, most of the data  
456 sets used to build these relationships between P fractions and soil order are from geomorphically  
457 stable landforms. In contrast, data from eroding hillslopes, regardless of soil order, show low  $P_{\text{apatite}}$

458 contributions to  $P_{\text{total}}$  (Fig. 8a). Consequently, neither soil residence time nor soil order is able to  
459 predict the low  $P_{\text{apatite}}$  contributions on eroding, soil-mantled hillslopes.

460 *Why do soil order and soil residence time fail to explain the contribution of  $P_{\text{apatite}}$ ?*

461 Whereas soil residence time on eroding hillslopes explains the dominance of soil orders  
462 typical of young geomorphic surfaces, it fails to account for the low contribution of  $P_{\text{apatite}}$  to  $P_{\text{total}}$ .

463 Soil order is determined largely by field observations of soil morphology including soil colour  
464 coatings, texture, structure, and horizons. The vertical depth distribution of these morphological  
465 properties is particularly diagnostic for several soil orders. For example, vertical distribution of soil  
466 texture and B horizon development are critical for determining a series of soils from Inceptisols to  
467 Ultisols (Soil Survey Staff, 2014). Continual mixing and/or consequent rejuvenation of a soil by  
468 erosion and soil production, for instance, would physically prevent the development of such vertical  
469 properties, similar to the effects of bioturbation (Johnson and Watson-Stegner, 1987). Because of this,  
470 soil orders characteristic for young geomorphic surfaces can develop from strongly weathered parent  
471 material as long as soil residence time is short and thus prevent significant vertical horizonation  
472 within the soils. It is also notable that the only soil order that is associated with mature soil  
473 development in Fig. 8a is the Oxisol. This is because in soil taxonomy, Oxisols, unlike Ultisols, do  
474 not require strong vertical stratification in clay contents and the classification is largely dependent on  
475 heavily-weathered soil minerals. The observation that soil order can be decoupled from weathering  
476 state of the parent material is not limited to eroding hillslopes. At the Cooloola sand dune soil  
477 chronosequence in Australia (Chen et al., 2015) (Fig. 8b), unlike at most other soil chronosequences,  
478 the young Entisols exhibits low levels of apatite P, simply because highly weathered sand deposits  
479 constitute the site's soil parent material.

480 The insensitivity of soil order to pre-weathering in parent material is consistent with our sites  
481 where Entisols and Inceptisols have formed from already chemically weathered saprolite. This is  
482 evident from the FR data (Fig. 4), where the soils have not formed from fresh bedrock but from  
483 saprolite overlying unweathered granodiorite. The saprolite weathering is evident by the dominance of

484 secondary P forms (Fig. 4) and enrichment in biogeochemically conservative elements such as Zr  
485 (Yoo et al., 2011). We did not reach the depth to fresh bedrock despite hand augering to depths of 2 to  
486 9 meters below the soil-saprolite boundary.

487 Therefore at least for eroding, soil mantled hillslopes, available data suggest that soil P  
488 dynamics neither proceed in tandem with the general developmental sequence of soil orders as  
489 proposed by Smeck (1985) nor make soil residence time a good predictor of soil P dynamics.

490 We believe the reason for the discrepancy between chronosequences and hillslopes is derived  
491 from a fundamental difference between ‘erosional’ soils and ‘depositional’ soils. In contrast to  
492 hillslope soils, most chronosequences are originally developed in relatively unweathered parent  
493 material of water-, and glacier-transported origin. These transport mechanisms usually comprise  
494 comminution and particle size sorting. Deposition of lighter and more weathered mineral particles  
495 (clays, oxides) in the lowlands becomes less likely since these particles offer less resistance to  
496 physical transport (Dellinger et al., 2014; Kautz and Martin, 2007). Instead, the less weathered  
497 particles of mostly larger size fractions (silt, sand, >2 mm) preferentially accumulate and ultimately  
498 form the parent material of lowland chronosequences (e.g., see parent material of chronosequence  
499 soils from NZ and California: Eger et al., 2011; Harden, 1987; Ross et al., 1977; Stevens, 1968; Wells  
500 and Goff, 2007).

501 Chronosequences that are formed from volcanic rocks, like in Hawaii (Crews et al., 1995;  
502 Vitousek, 2004), behave similar to chronosequences developed from sedimentary lithologies: lava  
503 flows in Hawaii create new, minimally eroding geomorphic surfaces from initially unweathered,  
504  $P_{\text{apatite}}$ -rich parent material, conceptually similar to chronosequences on sedimentary deposits that  
505 involve particle size-differentiating transport (Fig. 5). To our knowledge, the Cooloola coastal dune  
506 sequence is the only published soil chronosequence with P fractionation data derived from a pre-  
507 weathered allochthonous parent material. Not unlike our residence time gradients, it shows low and  
508 invariant  $P_{\text{apatite}}$  values across the entire sequence (Chen et al., 2015). Thus, both concepts, soil  
509 residence time and soil age in their narrow definitions do not consider any pre-weathering of parent

510 material. However, soil age is often able to structure the evolution of soils on chronosequences  
511 because the parent material at the start of soil formation is usually minimally weathered.

## 512 **Vertical distribution of P fractions**

513 It has been proposed (Porder et al., 2007a; Uhlig and von Blanckenburg, 2016) that a  
514 ‘vertically oriented’ version of the Walker and Syers (1976) model of P evolution applies to the  
515 changes of P fractions with depth (Fig. 9A). Such model recognises the inverse relationship between  
516 soil depth and mineral age following the incorporation of minerals into the active weathering zone of  
517 saprolite and soil.

518 However, the FR data and the review of existing studies allow this model to be modified at  
519 multiple fronts. In contrast to the expectation from the vertically oriented Walker and Syers model,  
520 total P does not gradually increase with increasing soil depth (Fig. 9B). Our data from FR (Fig. 4)  
521 indicate that total P decreases as bedrock chemically weathers to saprolite but that total P is greater in  
522 soils than in saprolite, albeit soil P dominated by secondary P forms. We attribute higher soil P  
523 concentrations to two processes: 1) dust deposition, and 2) biological nutrient redistribution (nutrient  
524 uplift) (Jobbágy and Jackson, 2004), whereby roots propagate into the saprolite and take up bio-  
525 available P from the saprolite zone. Plant-bound P is then returned to the soil as organic P, and partly  
526 transformed into other secondary (inorganic) P forms. Enrichment of P in surface soils associated with  
527 biological nutrient uptake and/or atmospheric deposition has been commonly observed (Chadwick  
528 and Asner, 2016; Merritts et al., 1992; Yoo et al., 2015) and does not seem to be necessarily limited to  
529 a particular P fraction or geomorphic setting (slopes vs. chronosequences) (Agbenin and Tiessen,  
530 1994; Homyak et al., 2014; Lajtha and Schlesinger, 1988; Mage and Porder, 2013; Stevens, 1968;  
531 Turner and Laliberté, 2015). Additionally, organic matter is concentrated in the top of the weathering  
532 profile which together with Fe/Al oxides and secondary silicate clays partly protects P from leaching  
533 through the formation of  $P_{org}$ ,  $P_{occ}$  and  $P_{Fe/Al}$ . With increasing depth, the P-depleted saprolite zone  
534 beneath the enriched soil will eventually transition into more unweathered parent material with higher  
535 P concentrations and an increase of  $P_{apatite}$ .

536 Therefore, it is not erosion directly that rejuvenates P. It is instead plant uptake of P at depth  
537 and dust deposition that rejuvenates soil P. Indirectly, erosion is required to maintain an ongoing  
538 supply of P to the root exploration zone of plants.

## 539 **Conclusion**

540 We characterised P fractionation in soils from eroding hillslopes across two soil residence  
541 time gradients and compared these new results against published soil P data from hillslopes and soil  
542 chronosequences on non-eroding landforms. We tested the Walker and Syers paradigm of soil P  
543 development as derived from soil chronosequences against hillslope soils through the conceptual link  
544 between soil residence times and soil ages. A naive application of this P model to eroding hillslopes  
545 predicts dominance of  $P_{\text{apatite}}$  over secondary P in soils with very short residence times. However, we  
546 find the majority of soil P we and others have measured exists in the form of secondary P (83-97% in  
547 our data) regardless of soil residence time. Furthermore, soil residence time also does not explain the  
548 distribution of the secondary P forms. We conclude that the fundamental difference between  
549 chronosequence and hillslope soil derives from the weathering occurring in the bedrock (formation of  
550 saprolite) before it becomes part of the mobile soil. During initial stages of chronosequence  
551 development  $P_{\text{apatite}}$  almost always dominates and P-depleted saprolite is normally not present. In  
552 contrast, on hillslopes weathered bedrock or saprolite appears to be common, combined with soils of  
553 short residence times and immature soil development. The legacy of pre-soil weathering of the  
554 underlying saprolite effectively counteracts the fertilising potential of the tectonic uplift – soil erosion  
555 – soil production feedback. Our data also indicate that plants may play an important role in  
556 redistributing P by uplift from the saprolite zone to the soil. Together with external dust, this  
557 redistribution increases soil P concentrations relative to the saprolite. Our work suggests that limits on  
558 ecosystem development through a decline of bio-available soil P forms may be more relevant to  
559 eroding hillslope soils than previously thought.

## 560 **Acknowledgements**

561 We thank the Department of Conservation for granting permission to sample soils in New Zealand.  
 562 AE, KY and PCA had the conceptual idea for the research, GB performed the majority of the P  
 563 laboratory analysis, XW prepared the samples and data from Feather River, AE and KY lead the data  
 564 interpretation and write-up with contributions of all co-authors. KY and SM designed and conducted  
 565 sampling at Feather River. IL and AE collected the New Zealand samples with support from NSF  
 566 (OISE-1015454 to IL). AE was partially supported through a Landcare Research Capability Fund  
 567 grant. KY thanks NSF (EAR-1253198) for supporting his portion of this work. KY and SM appreciate  
 568 help in the field from Beth Weinman, Martin Hurst, Manny Gabet, and Tony Dosseto. IL and AE are  
 569 grateful to Brendon Malcolm for help in the field.

## 570 **References**

- 571 Abekoe, M.K., Tiessen, H., 1998. Fertilizer P transformations and P availability in hillslope soils of  
 572 northern Ghana. *Nutrient Cycling in Agroecosystems* 52(1), 45-54.
- 573 Aciego, S.M., Riebe, C.S., Hart, S.C., Blakowski, M.A., Carey, C.J., Aarons, S.M., Dove, N.C., Botthoff,  
 574 J.K., Sims, K.W.W., Aronson, E.L., 2017. Dust outpaces bedrock in nutrient supply to montane  
 575 forest ecosystems. *Nat Commun* 8.
- 576 Agbenin, J.O., Tiessen, H., 1994. Phosphorus transformations in a toposequence of lithosols and  
 577 cambisols from semi-arid northeastern Brazil. *Geoderma* 62(4), 345-362.
- 578 Almond, P., Roering, J., Hales, T.C., 2007. Using soil residence time to delineate spatial and temporal  
 579 patterns of transient landscape response. *J Geophys Res-Earth* 112(F3).
- 580 Almond, P.C., Tonkin, P.J., 1999. Pedogenesis by upbuilding in an extreme leaching and weathering  
 581 environment, and slow loess accretion, South Westland, New Zealand. *Geoderma* 92(1-2), 1-  
 582 36.
- 583 Amundson, R., Heimsath, A., Owen, J., Yoo, K., Dietrich, W.E., 2015. Hillslope soils and vegetation.  
 584 *Geomorphology* 234(0), 122-132.
- 585 Araújo, M.S.B., Schaefer, C.E.R., Sampaio, E.V.S.B., 2004. Soil phosphorus fractions from  
 586 toposequences of semi-arid Latosols and Luvisols in northeastern Brazil. *Geoderma* 119(3-  
 587 4), 309-321.
- 588 Arvin, L.J., Riebe, C.S., Aciego, S.M., Blakowski, M.A., 2017. Global patterns of dust and bedrock  
 589 nutrient supply to montane ecosystems. *Science Advances* 3(12).
- 590 Attal, M., Mudd, S.M., Hurst, M.D., Weinman, B., Yoo, K., Naylor, M., 2015. Impact of change in  
 591 erosion rate and landscape steepness on hillslope and fluvial sediments grain size in the  
 592 Feather River basin (Sierra Nevada, California). *Earth Surf. Dynam.* 3(1), 201-222.
- 593 Blake, L., Johnston, A.E., Poulton, P.R., Goulding, K.W.T., 2003. Changes in soil phosphorus fractions  
 594 following positive and negative phosphorus balances for long periods. *Plant and Soil* 254(2),  
 595 245-261.
- 596 Blakemore, L.C., Searle, B.K., Daly, B.K.N., 1987. Methods for chemical analysis of soils. Soil Bureau  
 597 Scientific Report 80.
- 598 Boyle, J.F., Chiverrell, R.C., Norton, S.A., Plater, A.J., 2013. A leaky model of long-term soil  
 599 phosphorus dynamics. *Global Biogeochemical Cycles* 27(2), 516-525.
- 600 Chadwick, K.D., Asner, G.P., 2016. Tropical soil nutrient distributions determined by biotic and  
 601 hillslope processes. *Biogeochemistry* 127(2-3), 273-289.



- 602 Chadwick, O.A., Derry, L.A., Vitousek, P.M., Huebert, B.J., Hedin, L.O., 1999. Changing sources of  
603 nutrients during four million years of ecosystem development. *Nature* 397(6719), 491-497.
- 604 Chen, C.R., Hou, E.Q., Condrón, L.M., Bacon, G., Esfandbod, M., Olley, J., Turner, B.L., 2015. Soil  
605 phosphorus fractionation and nutrient dynamics along the Cooloola coastal dune  
606 chronosequence, southern Queensland, Australia. *Geoderma* 257–258, 4-13.
- 607 Condrón, L.M., Cornforth, I.S., Davis, M.R., Newman, R.H., 1996. Influence of conifers on the forms  
608 of phosphorus in selected New Zealand grassland soils. *Biology and Fertility of Soils* 21(1),  
609 37-42.
- 610 Crews, T.E., Kitayama, K., Fownes, J.H., Riley, R.H., Herbert, D.A., Mueller-Dombois, D., Vitousek,  
611 P.M., 1995. Changes in Soil Phosphorus Fractions and Ecosystem Dynamics across a Long  
612 Chronosequence in Hawaii. *Ecology* 76(5), 1407-1424.
- 613 Cross, A.F., Schlesinger, W.H., 1995. A literature review and evaluation of the Hedley fractionation:  
614 Applications to the biogeochemical cycle of soil phosphorus in natural ecosystems.  
615 *Geoderma* 64(3–4), 197-214.
- 616 Dellinger, M., Gaillardet, J., Bouchez, J., Calmels, D., Galy, V., Hilton, R.G., Louvat, P., France-Lanord,  
617 C., 2014. Lithium isotopes in large rivers reveal the cannibalistic nature of modern  
618 continental weathering and erosion. *Earth and Planetary Science Letters* 401, 359-372.
- 619 Dere, A.L., White, T.S., April, R.H., Reynolds, B., Miller, T.E., Knapp, E.P., McKay, L.D., Brantley, S.L.,  
620 2013. Climate dependence of feldspar weathering in shale soils along a latitudinal gradient.  
621 *Geochimica et Cosmochimica Acta* 122, 101-126.
- 622 Dick, W.A., Tabatabai, M.A., 1977. Determination of orthophosphate in aqueous solutions containing  
623 labile organic and inorganic phosphorus compounds. *Journal of Environmental Quality* 6(1).
- 624 Dixon, J.L., Heimsath, A.M., Amundson, R., 2009. The critical role of climate and saprolite weathering  
625 in landscape evolution. *Earth Surface Processes and Landforms* 34(11), 1507-1521.
- 626 Eger, A., Almond, P.C., Condrón, L.M., 2011. Pedogenesis, soil mass balance, phosphorus dynamics  
627 and vegetation communities across a Holocene soil chronosequence in a super-humid  
628 climate, South Westland, New Zealand. *Geoderma* 163(3-4), 185-196.
- 629 Eger, A., Almond, P.C., Condrón, L.M., 2013a. Phosphorus fertilization by active dust deposition in a  
630 super-humid, temperate environment—Soil phosphorus fractionation and accession  
631 processes. *Global Biogeochemical Cycles* 27(1), 108-118.
- 632 Eger, A., Almond, P.C., Wells, A., Condrón, L.M., 2013b. Quantifying ecosystem rejuvenation: foliar  
633 nutrient concentrations and vegetation communities across a dust gradient and a  
634 chronosequence. *Plant and Soil* 367(1), 93-109.
- 635 Filippelli, G.M., 2002. The Global Phosphorus Cycle. *Reviews in Mineralogy and Geochemistry* 48(1),  
636 391-425.
- 637 Frossard, E., Condrón, L.M., Oberson, A., Sinaj, S., Fardeau, J.C., 2000. Processes Governing  
638 Phosphorus Availability in Temperate Soils. *Journal of Environmental Quality* 29(1).
- 639 Gabet, E.J., Mudd, S.M., Milodowski, D.T., Yoo, K., Hurst, M.D., Dosseto, A., 2015. Local topography  
640 and erosion rate control regolith thickness along a ridgeline in the Sierra Nevada, California.  
641 *Earth Surface Processes and Landforms* 40(13), 1779-1790.
- 642 Gilbert, G.K., 1877. Report on the geology of the Henry Mountains, Washington, D.C.
- 643 Green, E.G., Dietrich, W.E., Banfield, J.F., 2006. Quantification of chemical weathering rates across  
644 an actively eroding hillslope. *Earth and Planetary Science Letters* 242(1-2), 155-169.
- 645 Guo, F., Yost, R.S., 1998. Partitioning Soil Phosphorus Into Three Discrete Pools of Differing  
646 Availability. *Soil Science* 163(10), 822-833.
- 647 Hahm, W.J., Riebe, C.S., Lukens, C.E., Araki, S., 2014. Bedrock composition regulates mountain  
648 ecosystems and landscape evolution. *Proceedings of the National Academy of Sciences*  
649 111(9), 3338-3343.
- 650 Harden, J.W., 1987. Soils developed in granitic alluvium near Merced, California. 1590A.
- 651 Heimsath, A.M., Dietrich, W.E., Nishiizumi, K., Finkel, R.C., 1997. The soil production function and  
652 landscape equilibrium. *Nature* 388(6640), 358-361.

- 653 Hilton, R.G., Galy, A., Hovius, N., 2008. Riverine particulate organic carbon from an active mountain  
654 belt: Importance of landslides. *Global Biogeochemical Cycles* 22(1), GB1017.
- 655 Homyak, P.M., Sickman, J.O., Melack, J.M., 2014. Pools, transformations, and sources of P in high-  
656 elevation soils: Implications for nutrient transfer to Sierra Nevada lakes. *Geoderma* 217–218,  
657 65-73.
- 658 Hovius, N., Stark, C.P., Allen, P.A., 1997. Sediment flux from a mountain belt derived by landslide  
659 mapping. *Geology* 25(3), 231-234.
- 660 Hurst, M.D., Mudd, S.M., Walcott, R., Attal, M., Yoo, K., 2012. Using hilltop curvature to derive the  
661 spatial distribution of erosion rates. *Journal of Geophysical Research: Earth Surface* 117(F2),  
662 n/a-n/a.
- 663 Izquierdo, J.E., Houlton, B.Z., van Huysen, T.L., 2013. Evidence for progressive phosphorus limitation  
664 over long-term ecosystem development: Examination of a biogeochemical paradigm. *Plant  
665 and Soil* 367(1), 135-147.
- 666 Jobbágy, E.G., Jackson, R.B., 2004. The uplift of soil nutrients by plants: biogeochemical  
667 consequences across scales. *Ecology* 85(9), 2380-2389.
- 668 Johnson, D.L., Watson-Stegner, D., 1987. Evolution model of pedogenesis. *Soil Science* 143(5), 349-  
669 366.
- 670 Kautz, C.Q., Martin, C.E., 2007. Chemical and physical weathering in New Zealand's Southern Alps  
671 monitored by bedload sediment major element composition. *Applied Geochemistry* 22(8),  
672 1715-1735.
- 673 Korup, O., McSaveney, M.J., Davies, T.R.H., 2004. Sediment generation and delivery from large  
674 historic landslides in the Southern Alps, New Zealand. *Geomorphology* 61(1–2), 189-207.
- 675 Lajtha, K., Schlesinger, W.H., 1988. The Biogeochemistry of Phosphorus Cycling and Phosphorus  
676 Availability Along a Desert Soil Chronosequence. *Ecology* 69(1), 24-39.
- 677 Larsen, I.J., Almond, P.C., Eger, A., Stone, J.O., Montgomery, D.R., Malcolm, B., 2014a. Rapid Soil  
678 Production and Weathering in the Southern Alps, New Zealand. *Science* 343(6171), 637-640.
- 679 Larsen, I.J., Montgomery, D.R., Greenberg, H.M., 2014b. The contribution of mountains to global  
680 denudation. *Geology*.
- 681 Lebedeva, M.I., Fletcher, R.C., Brantley, S.L., 2010. A mathematical model for steady-state regolith  
682 production at constant erosion rate. *Earth Surface Processes and Landforms* 35(5), 508-524.
- 683 Little, T.A., Cox, S., Vry, J.K., Batt, G., 2005. Variations in exhumation level and uplift rate along the  
684 obliqu-slip Alpine fault, central Southern Alps, New Zealand. *Geological Society of America  
685 Bulletin* 117(5-6), 707-723.
- 686 Mage, S.M., Porder, S., 2013. Parent Material and Topography Determine Soil Phosphorus Status in  
687 the Luquillo Mountains of Puerto Rico. *Ecosystems* 16(2), 284-294.
- 688 Marx, S.K., McGowan, H.A., Kamber, B.S., 2009. Long-range dust transport from eastern Australia: A  
689 proxy for Holocene aridity and ENSO-type climate variability. *Earth and Planetary Science  
690 Letters* 282(1-4), 167-177.
- 691 McClintock, M.A., Brocard, G., Willenbring, J., Tamayo, C., Porder, S., Pett-Ridge, J.C., 2015. Spatial  
692 variability of African dust in soils in a montane tropical landscape in Puerto Rico. *Chemical  
693 Geology* 412, 69-81.
- 694 Merritts, D.J., Chadwick, O.A., Hendricks, D.M., Brimhall, G.H., Lewis, C.J., 1992. The Mass Balance of  
695 Soil Evolution on Late Quaternary Marine Terraces, Northern California. *Geological Society  
696 of America Bulletin* 104(11), 1456-1470.
- 697 Milodowski, D.T., Mudd, S.M., Mitchard, E.T.A., 2014. Erosion rates as a potential bottom-up control  
698 of forest structural characteristics in the Sierra Nevada Mountains. *Ecology* 96(1), 31-38.
- 699 Milodowski, D.T., Mudd, S.M., Mitchard, E.T.A., 2015. Topographic roughness as a signature of the  
700 emergence of bedrock in eroding landscapes. *Earth Surf. Dynam.* 3(4), 483-499.
- 701 Mudd, S.M., Yoo, K., 2010. Reservoir theory for studying the geochemical evolution of soils. *J  
702 Geophys Res-Earth* 115.

## Soil erosion and phosphorus

- 703 Murphy, J., Riley, J.P., 1962. A modified single solution method for the determination of phosphate  
704 in natural waters. *Analytica Chimica Acta* 27, 31-36.
- 705 Nelson, D.L., Nelson, D.L., Lehninger, A.L., Cox, M.M., 2008. *Lehninger principles of biochemistry*.  
706 W.H. Freeman, New York.
- 707 NIWA, 2016. National Climate Database. New Zealand National Institute of Water and Atmospheric  
708 Research.
- 709 Olsen, S.R., Sommers, L.E., 1982. Determination of available phosphorus. In: A.L. Page, R.H. Miller,  
710 D.R. Keeney (Eds.), *Method of Soil Analysis*. American Society of Agronomy, Madison, WI,  
711 pp. 403.
- 712 Paytan, A., McLaughlin, K., 2007. The Oceanic Phosphorus Cycle. *Chemical Reviews* 107(2), 563-576.
- 713 Peltzer, D.A., Wardle, D.A., Allison, V.J., Baisden, W.T., Bardgett, R.D., Chadwick, O.A., Condon, L.M.,  
714 Parfitt, R.L., Porder, S., Richardson, S.J., Turner, B.L., Vitousek, P.M., Walker, J., Walker, L.R.,  
715 2010. Understanding ecosystem retrogression. *Ecological Monographs* 80(4), 509-529.
- 716 Porder, S., Hilley, G., 2011. Linking chronosequences with the rest of the world: predicting soil  
717 phosphorus content in denuding landscapes. *Biogeochemistry* 102(1), 153-166.
- 718 Porder, S., Hilley, G.E., Chadwick, O.A., 2007a. Chemical weathering, mass loss, and dust inputs  
719 across a climate by time matrix in the Hawaiian Islands. *Earth and Planetary Science Letters*  
720 258(3-4), 414-427.
- 721 Porder, S., Ramachandran, S., 2013. The phosphorus concentration of common rocks—a potential  
722 driver of ecosystem P status. *Plant and Soil* 367(1), 41-55.
- 723 Porder, S., Vitousek, P., Chadwick, O., Chamberlain, C., Hilley, G., 2007b. Uplift, Erosion, and  
724 Phosphorus Limitation in Terrestrial Ecosystems. *Ecosystems* 10(1), 159-171.
- 725 R Core Team, 2017. R: A language and environment for statistical computing. R Foundation for  
726 Statistical Computing, Vienna.
- 727 Richardson, S., Peltzer, D., Allen, R., McGlone, M., Parfitt, R., 2004. Rapid development of  
728 phosphorus limitation in temperate rainforest along the Franz Josef soil chronosequence.  
729 *Oecologia* 139(2), 267-276.
- 730 Riebe, C.S., Kirchner, J.W., Finkel, R.C., 2003. Long-term rates of chemical weathering and physical  
731 erosion from cosmogenic nuclides and geochemical mass balance. *Geochimica et*  
732 *Cosmochimica Acta* 67(22), 4411-4427.
- 733 Riebe, C.S., Kirchner, J.W., Granger, D.E., Finkel, R.C., 2000. Erosional equilibrium and disequilibrium  
734 in the Sierra Nevada, inferred from cosmogenic <sup>26</sup>Al and <sup>10</sup>Be in alluvial sediment. *Geology*  
735 28(9), 803-806.
- 736 Ross, C.W., Mew, G., Searle, P.L., 1977. Soil sequences on two terrace systems in the North Westland  
737 area, New Zealand. *N. Z. Journal of Science* 20, 231-244.
- 738 Saucedo, G.J., Wagner, D.L., 1992. Geologic map of the Chico quadrangle, Regional Geologic Map 7A.  
739 California Division of Mines and Geology.
- 740 Saunders, W.M.H., Williams, E.G., 1955. Observations on the determination of total organic  
741 phosphorus in soils. *Journal of Soil Science* 6(2), 254-267.
- 742 Selmants, P.C., Hart, S.C., 2010. Phosphorus and soil development: Does the Walker and Syers model  
743 apply to semiarid ecosystems? *Ecology* 91(2), 474-484.
- 744 Smeck, N.E., 1985. Phosphorus dynamics in soils and landscapes. *Geoderma* 36(3), 185-199.
- 745 Smith, B.F.L., Bain, B.C., 1982. A sodium hydroxide fusion method for the determination of total  
746 phosphate in soils. *Communications in Soil Science and Plant Analysis* 13(3), 185-190.
- 747 Soil Survey Staff, 2014. *Keys to Soil Taxonomy*. 12 ed. USDA-Natural Resources Conservation Service,  
748 Washington, DC.
- 749 Stevens, P.R., 1968. A chronosequence of soils near the Franz Josef Glacier, University of Canterbury,  
750 Lincoln, 389 pp.
- 751 Tiessen, H., Moir, J.O., 1993. Characterization of available P by sequential extraction. In: M.R. Carter,  
752 E.G. Gregorich (Eds.), *Soil sampling and methods of analysis*. Canadian Society of Soil  
753 Science.

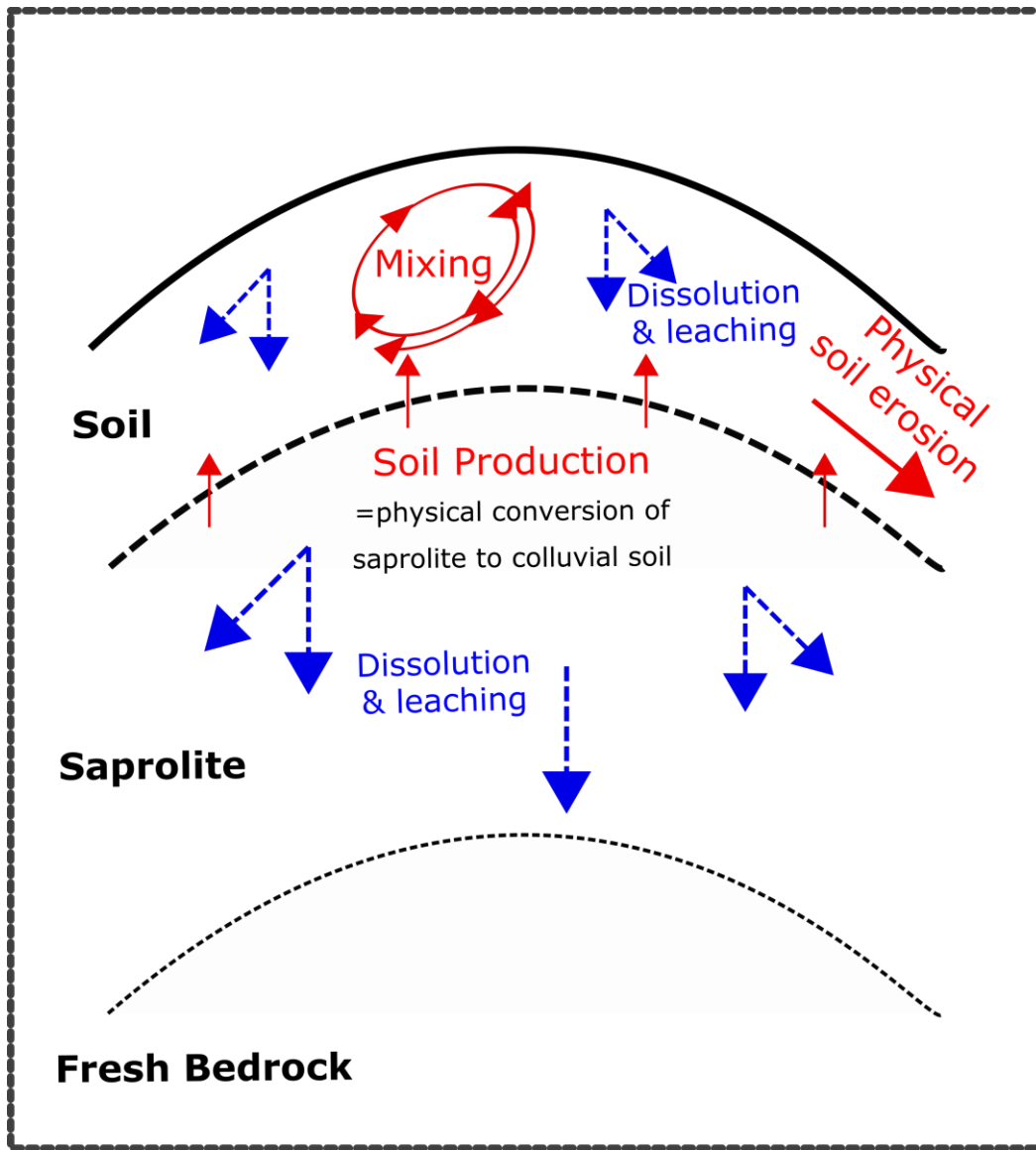
- 754 Tippet, J.M., Kamp, P.J.J., 1993. Fission track analysis of the Late Cenozoic vertical kinematics of  
755 continental pacific crust, South Island, New Zealand. *Journal of Geophysical Research: Solid*  
756 *Earth* 98(B9), 16119-16148.
- 757 Tonkin, P.J., Basher, L.R., 2001. Soil chronosequences in subalpine superhumid Cropp Basin, western  
758 Southern Alps, New Zealand. *New Zealand Journal of Geology and Geophysics* 44(1), 37-45.
- 759 Turner, B., Laliberté, E., 2015. Soil Development and Nutrient Availability Along a 2 Million-Year  
760 Coastal Dune Chronosequence Under Species-Rich Mediterranean Shrubland in  
761 Southwestern Australia. *Ecosystems* 18(2), 287-309.
- 762 Turner, B.L., Condron, L.M., 2013. Pedogenesis, nutrient dynamics, and ecosystem development: the  
763 legacy of TW Walker and JK Syers. *Plant and Soil* 367(1-2), 1-10.
- 764 Uhlig, D., von Blanckenburg, F., 2016. Deep subsoil tree phosphorus sources in forest ecosystems,  
765 Goldschmidt 2016. European Association of Geochemistry and Geochemical Society,  
766 Yokohama.
- 767 Vitousek, P., Chadwick, O., Matson, P., Allison, S., Derry, L., Kettley, L., Luers, A., Mecking, E.,  
768 Monasta, V., Porder, S., 2003. Erosion and the Rejuvenation of Weathering-derived  
769 Nutrient Supply in an Old Tropical Landscape. *Ecosystems* 6(8), 762-772.
- 770 Vitousek, P.M., 2004. *Nutrient Cycling and Limitation*. Princeton Environmental Institute Series.  
771 Princeton University Press, Princeton.
- 772 Wakabayashi, J., Sawyer, T.L., 2001. Stream Incision, Tectonics, Uplift, and Evolution of Topography  
773 of the Sierra Nevada, California. *The Journal of Geology* 109(5), 539-562.
- 774 Walker, T.W., Syers, J.K., 1976. The fate of phosphorus during pedogenesis. *Geoderma* 15(1), 1-19.
- 775 Wang, X., Yoo, K., Mudd, S.M., Weinman, B., Gutknecht, J., Gabet, E.J., 2018. Storage and export of  
776 soil carbon and mineral surface area along an erosional gradient in the Sierra Nevada,  
777 California. *Geoderma* 321, 151-163.
- 778 Wardle, P., 1977. Plant communities of Westland National Park (New Zealand) and neighbouring  
779 lowland and coastal areas. *New Zealand Journal of Botany* 15(2), 323-398.
- 780 Wells, A., Goff, J., 2007. Coastal dunes in Westland, New Zealand, provide a record of paleoseismic  
781 activity on the Alpine fault. *Geology* 35(8), 731-734.
- 782 Whitehouse, I.E., 1988. Geomorphology of the central Souther Alps, New Zealand: the interaction of  
783 plate collision and atmospheric circulation. *Z. Geomorph. N.F. Supp* 69, 105-116.
- 784 Yang, X., Post, W.M., 2011. Phosphorus transformations as a function of pedogenesis: A synthesis of  
785 soil phosphorus data using Hedley fractionation method. *Biogeosciences* 8(10), 2907-2916.
- 786 Yoo, K., Fisher, B., Ji, J.L., Aufdenkampe, A., Klaminder, J., 2015. The geochemical transformation of  
787 soils by agriculture and its dependence on soil erosion: An application of the geochemical  
788 mass balance approach. *Sci Total Environ* 521, 326-335.
- 789 Yoo, K., Mudd, S.M., 2008. Discrepancy between mineral residence time and soil age: Implications  
790 for the interpretation of chemical weathering rates. *Geology* 36(1), 35-38.
- 791 Yoo, K., Weinman, B., Mudd, S.M., Hurst, M., Attal, M., Maher, K., 2011. Evolution of hillslope soils:  
792 The geomorphic theater and the geochemical play. *Applied Geochemistry* 26, Supplement,  
793 S149-S153.
- 794 Zemunik, G., Turner, B.L., Lambers, H., Laliberté, E., 2015. Diversity of plant nutrient-acquisition  
795 strategies increases during long-term ecosystem development. *Nature Plants* 1, 15050.

796

797

798

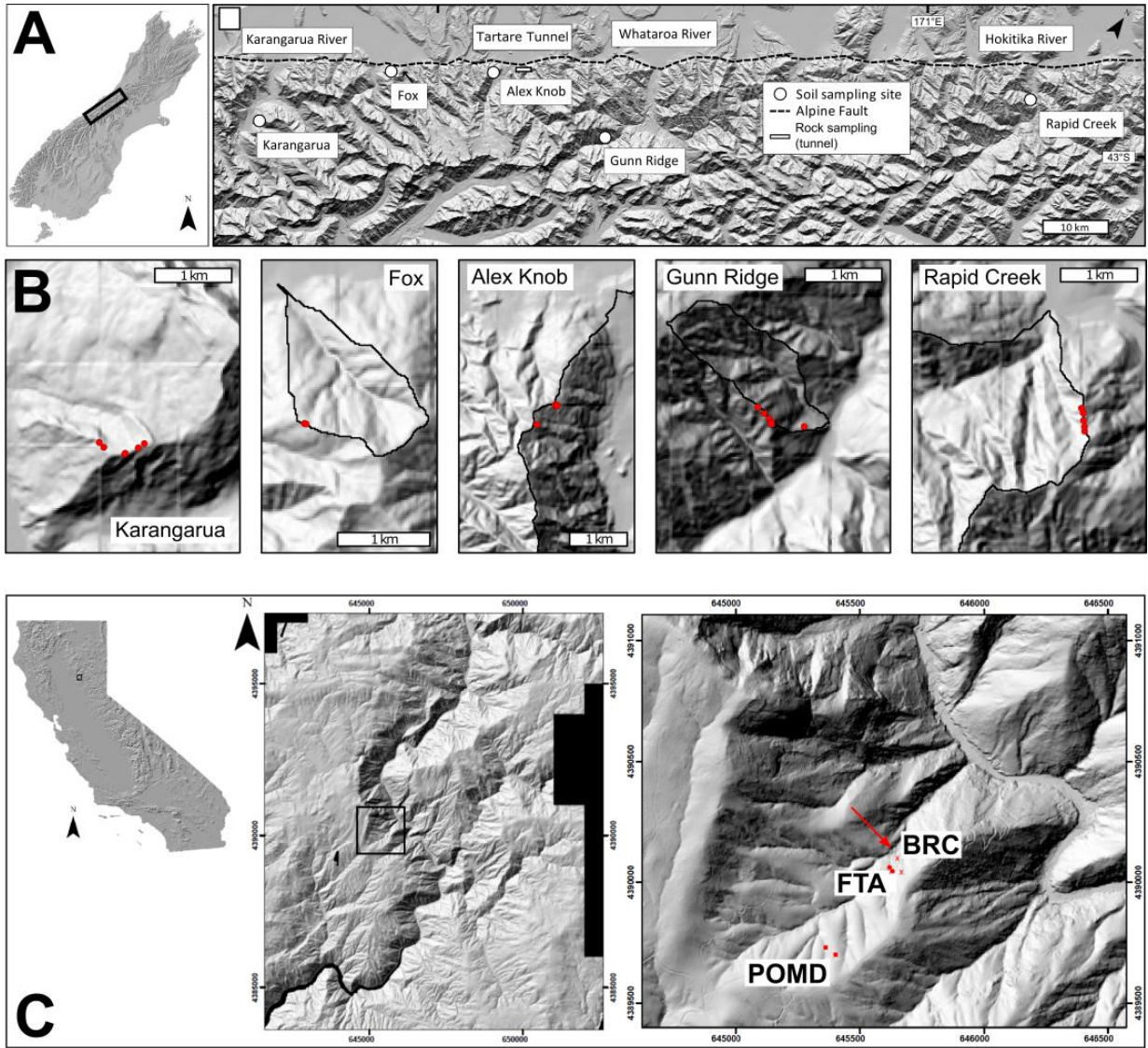
799



800

801 Fig. 1

# Soil erosion and phosphorus

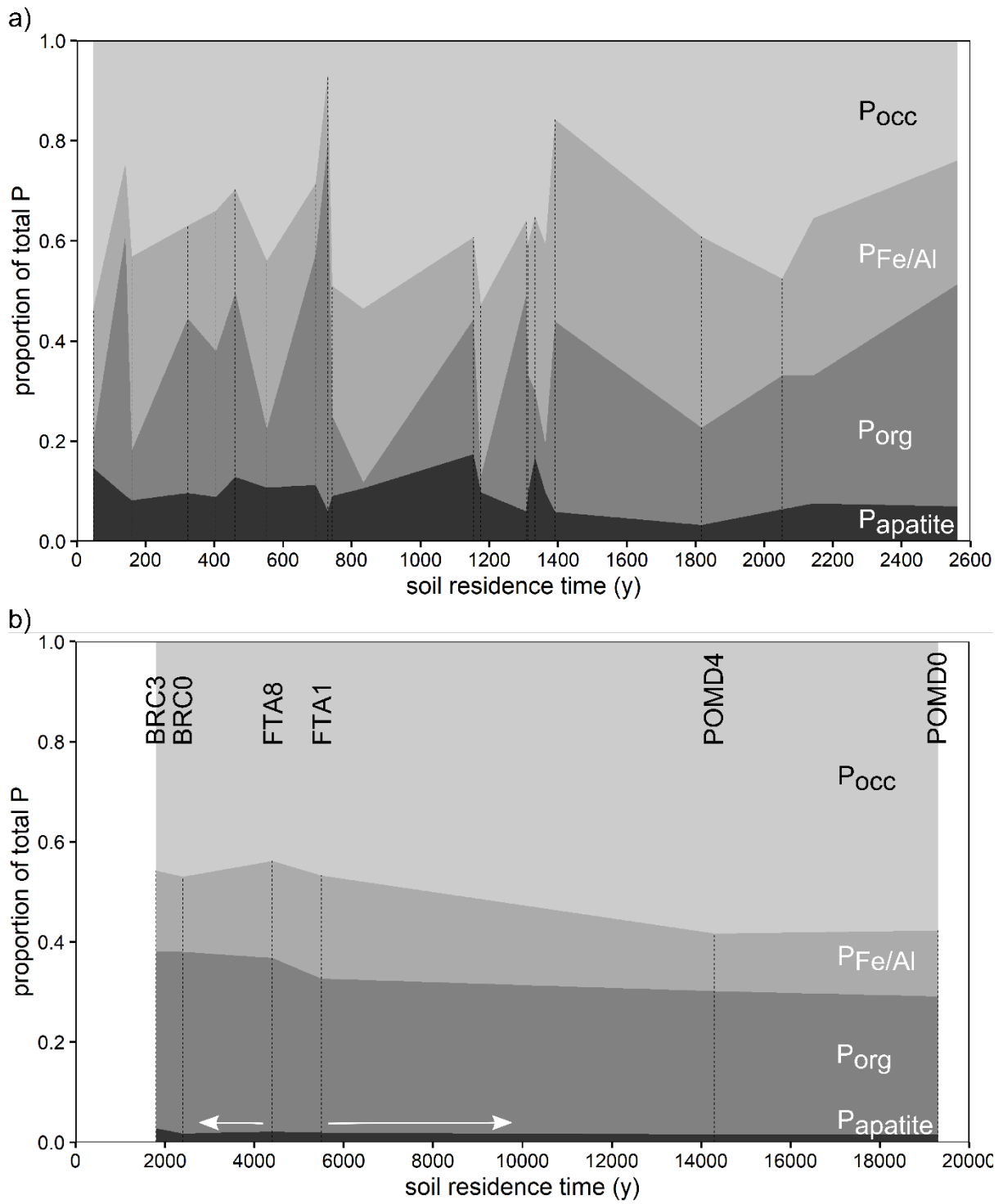


802

803 Fig. 2

804

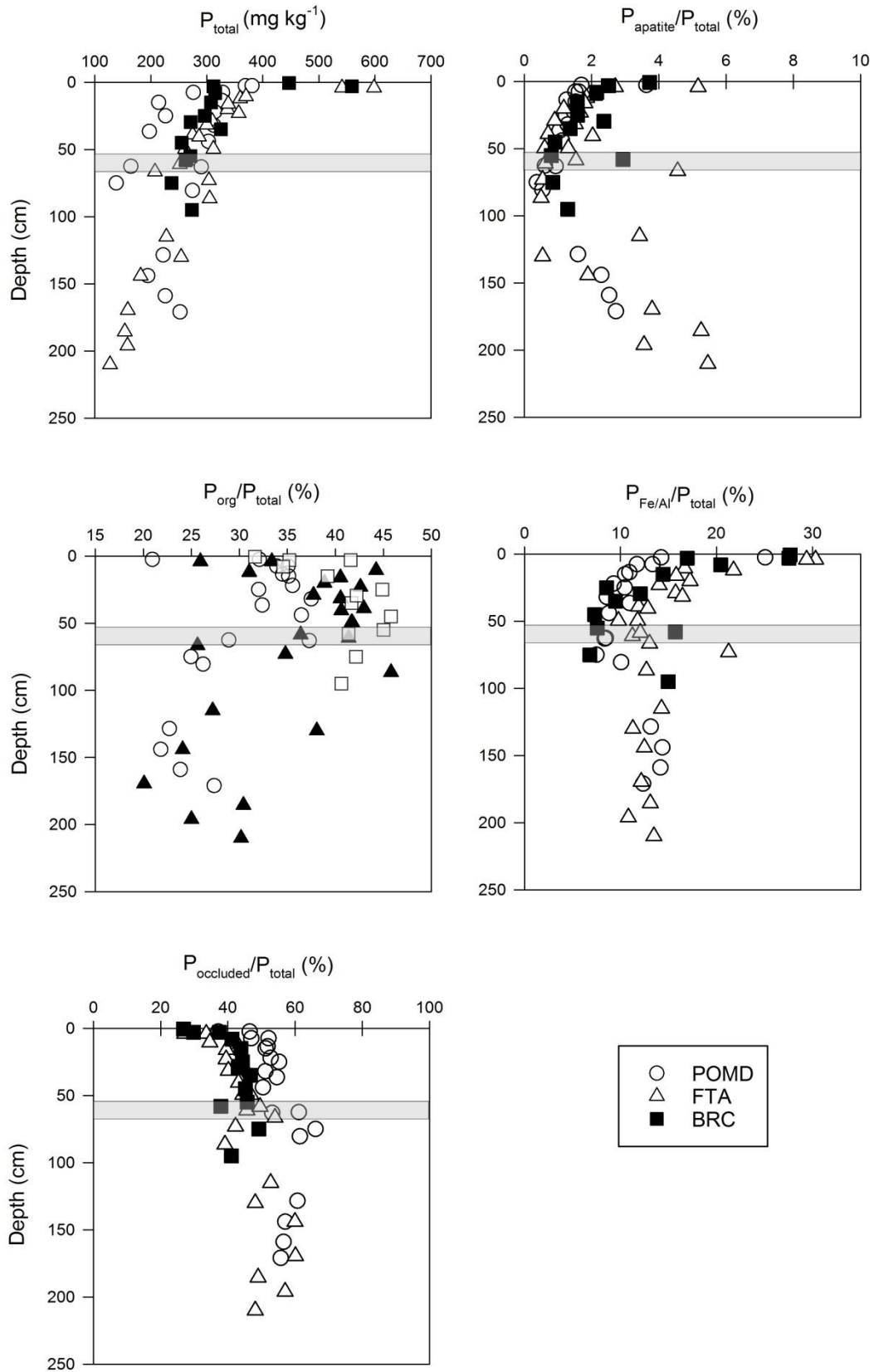
Soil erosion and phosphorus



805

806 Fig. 3

# Soil erosion and phosphorus

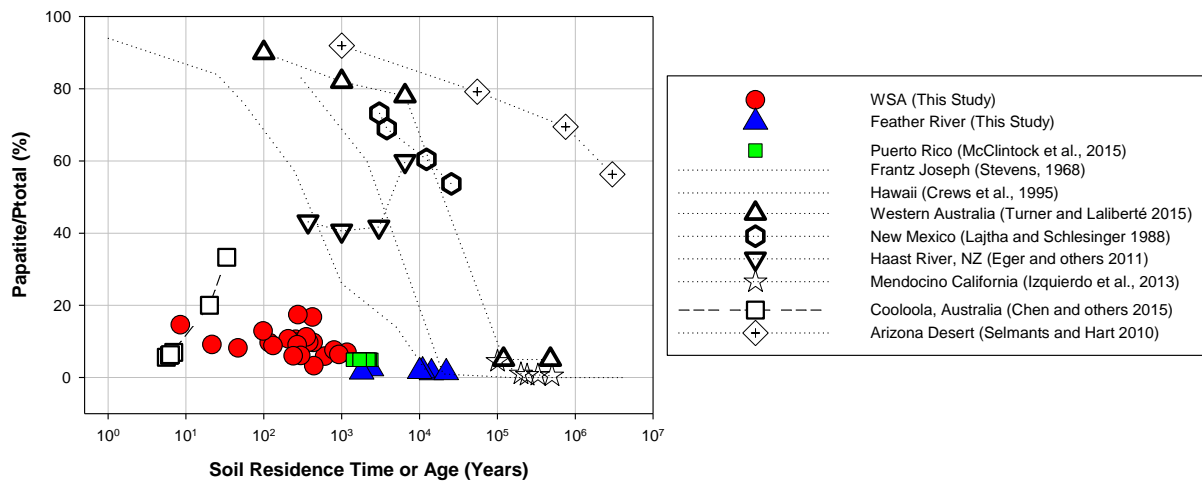


807

808 Fig. 4

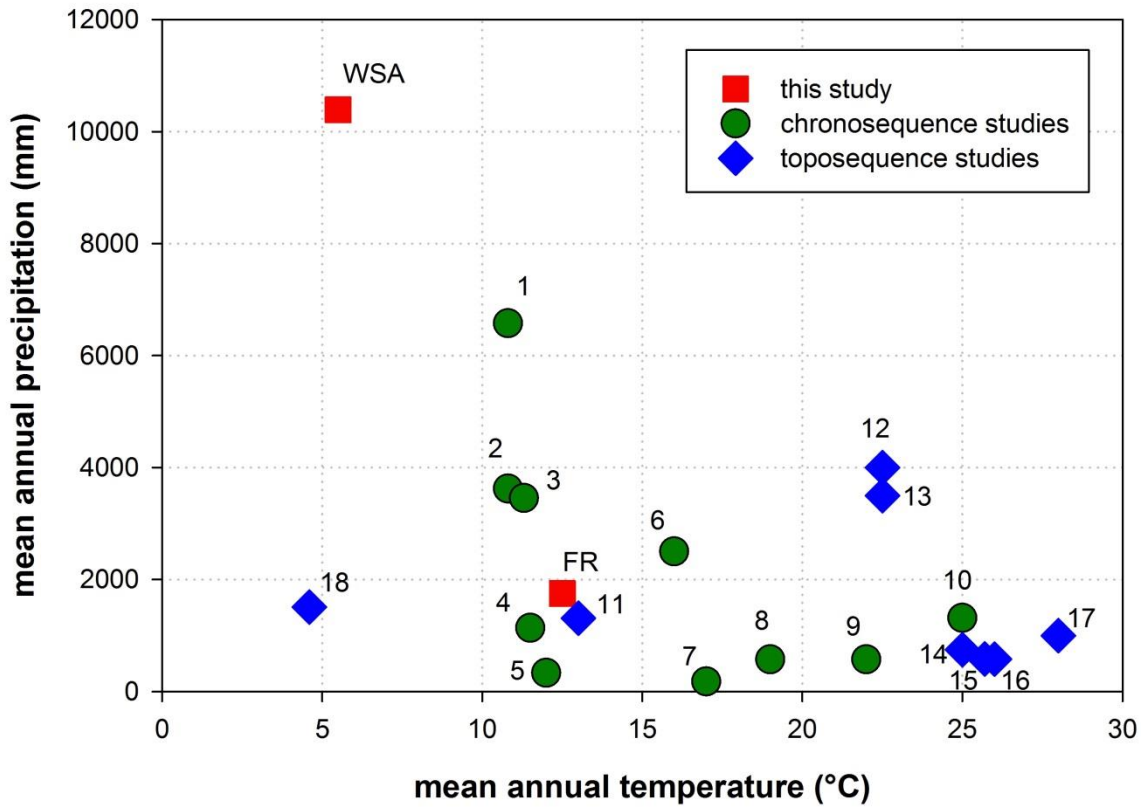


## Soil erosion and phosphorus



809

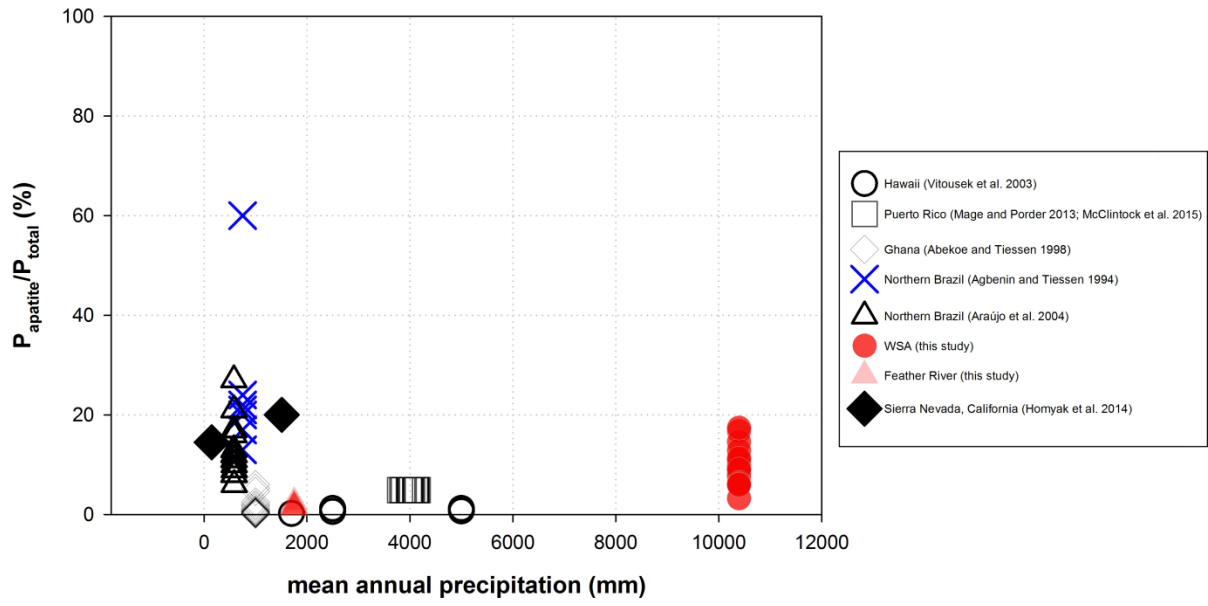
810 Fig. 5



811

812 Fig. 6

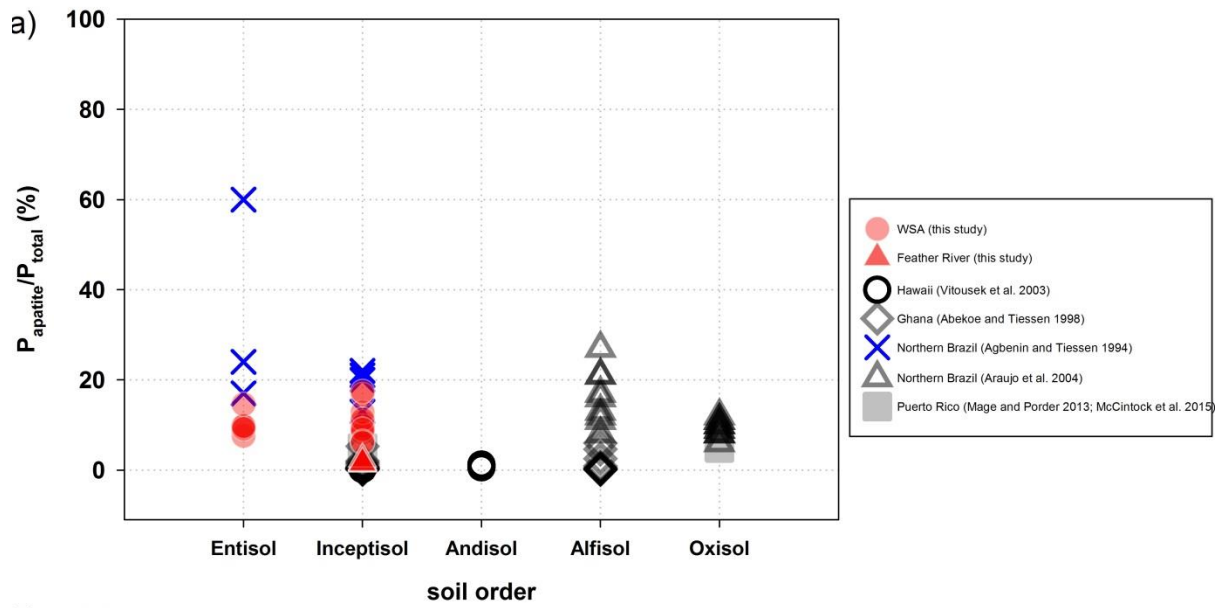
# Soil erosion and phosphorus



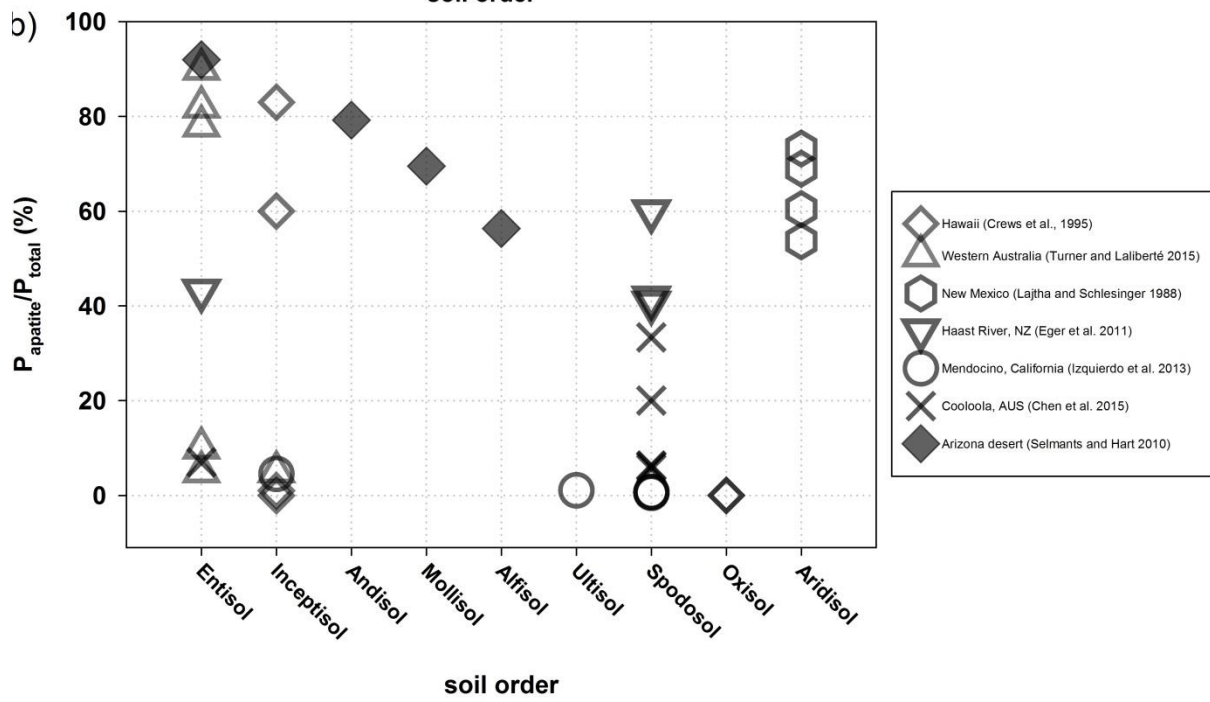
813

814 Fig. 7

## Soil erosion and phosphorus



815



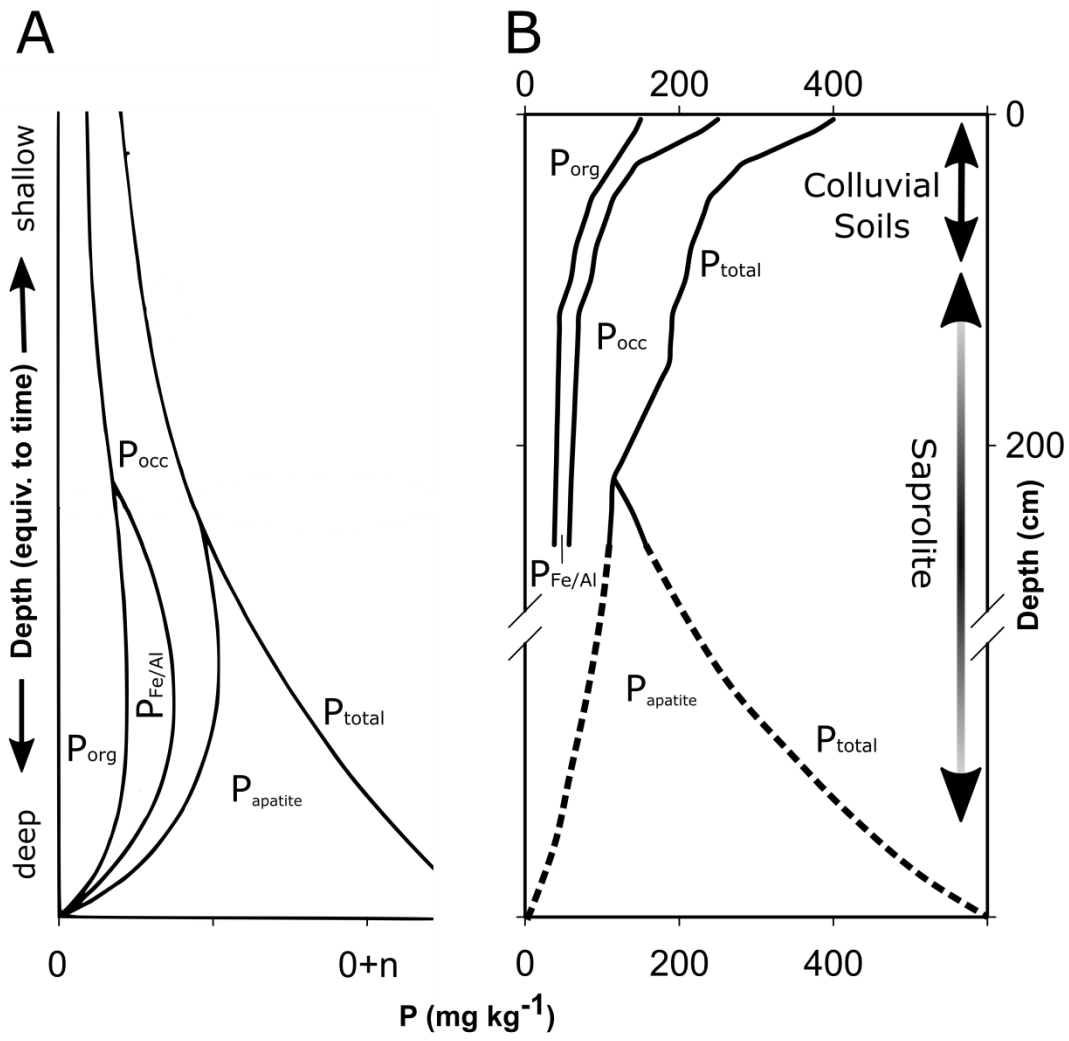
816

817 Fig. 8

818

819

820



821

822 Fig. 9

823

824

825 Fig. 1: Simplified conceptual model of hillslope processes affecting soils at steady-state soil thickness.

826 See text for detailed discussion.

827 Fig. 2: Locations of the study areas in the western Southern Alps/New Zealand (WSA) and the

828 Feather River/Northern Sierra Nevada, USA (FR). A) overview of the sample locations of the WSA

829 sites; B) detailed setting of each WSA soil pit on local ridge positions; C) overview and sample

830 locations of the FR sites. The arrow in C) indicates the current position of the knick point.

831 Fig. 3: Relative contributions of soil P fractions to  $P_{\text{total}}$  in a) WSA soils and b) FR soils as a function

832 of soil residence times. Dotted lines indicate the individual sites across the gradients. The white

833 arrows in b) indicate the potential range of soil residence time of the FTA sites as intermediate

834 between the BRC and POMD values. The FTA soil residence times are used for illustration purposes

835 are derived from the average of the erosion rates of  $35.7 \text{ mm ky}^{-1}$  (POMD) and  $250 \text{ mm ky}^{-1}$  (BRC).

836 Soil residence time has little influence on P fractions and secondary P fractions clearly dominate over

837  $P_{\text{apatite}}$  at all times.

838 Fig. 4: Depth profiles of soil P fractions relative to  $P_{\text{total}}$  at the FR sites. The grey bands indicate the

839 depths of soil-saprolite boundaries observed at the FR sites. The general decline of concentrations

840 with depth toward the saprolite appears to be a uniform feature independent of the soil residence time.

841 Only  $P_{\text{apatite}}$  increases again below 150 cm. See Table 2 for individual values.

842 Fig. 5: Relative contributions of  $P_{\text{apatite}}$  to  $P_{\text{total}}$  across soil residence time and soil age gradients (filled

843 solid points denote studies on hillslope soils, whereas hollow points are chronosequence studies).

844 Fig. 6: Climate data from the sites discussed in this study (Fig. 8 and 9). References as follows: 1, 2

845 Franz Josef, NZ (Richardson et al., 2004) 3 Haast River, NZ (Eger et al., 2011); 4 Mendocino,

846 California (Izquierdo et al., 2013); 5 Arizona desert (Selmants and Hart, 2010); 6 Hawaii (Crews et

847 al., 1995); 7 New Mexico (Lajtha and Schlesinger, 1988); 8, 9 Western Australia (Turner and

848 Laliberté, 2015); 10 Northern Brazil (Agbenin and Tiessen, 1994); 11 Hawaii (Vitousek et al., 2003);

849 12 Puerto Rico (McClintock et al., 2015); 13 Puerto Rico (Mage and Porder, 2013); 14 Cooloola,

850 AUS (Chen et al., 2015); 15, 16 Northern Brazil (Araújo et al., 2004); 17 Ghana (Abekoe and Tiessen,  
851 1998); 18 Sierra Nevada, California (Homyak et al., 2014)

852 Fig. 7: Contribution of  $P_{\text{apatite}}$  to  $P_{\text{total}}$  versus mean annual precipitation for eroding hillslope soils from  
853 this study and from the literature. In plotting published data, we did not attempt to average the  
854 reported values or combine results from different depths for calculating soil profile integrated values.  
855 Instead all of the reported values are included in this figure. For the study conducted in the high Sierra  
856 Nevada (Homyak et al., 2014), we note that their reported P values are averaged over several soil  
857 profiles that include soils on hillslopes and adjacent depositional settings.

858 Fig. 8: Soil  $P_{\text{apatite}}/P_{\text{total}}$  plotted against soil orders for a) eroding hillslopes, and b) soil  
859 chronosequences.

860 Fig. 9: A) Vertically oriented Walker and Syers model and B) a new P dynamics model for  
861 weathering profiles based on the results from the Feather River sites. The WSA data show a similar  
862 pattern but lack the same detailed depth resolution due to the different sampling protocols. Although,  
863 we did not measure  $P_{\text{total}}$  for fresh bedrock at the Feather River, globally compiled P contents of  
864 ganodiorite bedrock types show mean value of  $810 \text{ mg kg}^{-1}$  with 25% value of 480 and 75 % value of  
865  $1004 \text{ mg kg}^{-1}$  (Porder and Ramachandran, 2013).

## Soil erosion and phosphorus

866 Table 1: Soil data for the WSA sites.

867 Table 2: Soil and saprolite data for the FR sites. The detailed and simplified P fractionations are  
868 shown. Note the residence time for BRC and POMD soils. No absolute residence time was calculated  
869 for the intermediate site.